

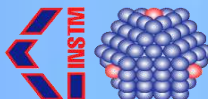
Magnetic Nanoparticles: recent advances in biomedical applications

P. Arosio

Dipartimento di Fisica and INSTM, Università degli studi di Milano, Milano (Italy)



UNIVERSITÀ DEGLI STUDI DI MILANO
DIPARTIMENTO DI FISICA



OUTLINE

- Brief intro to **MNPs**
- State of art for the Bio-Med applications (more insight into **MFH**)
- Focus on **NMR relaxometry (for clinical MRI)**:
 - Basic concepts
 - Reality vs Ideality
 - Several examples of our research
- Conclusions

What kind of magnetic nanoparticles we're talking about ?

Simplest (and mainly) form :

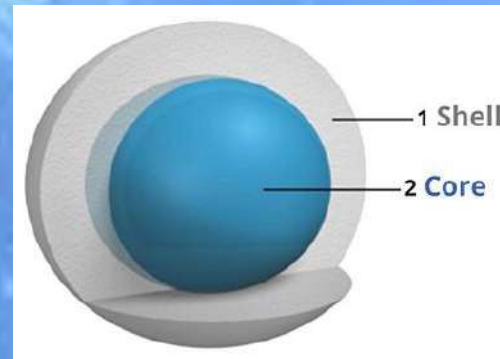
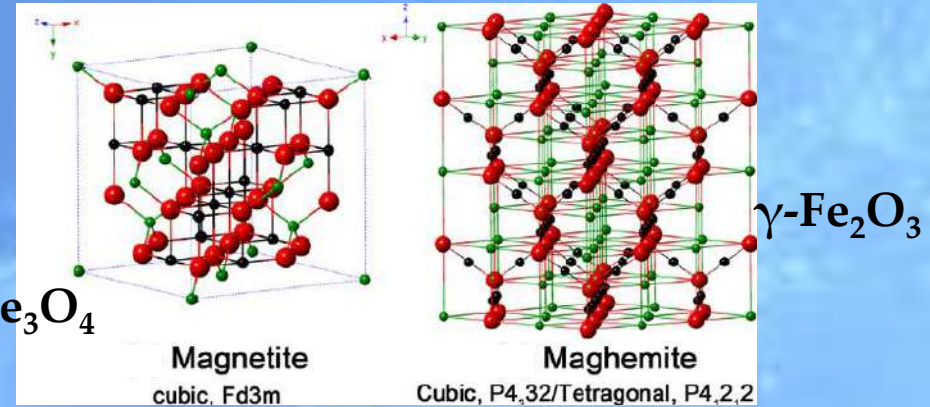
magnetic core
(often simple ferrites)

+

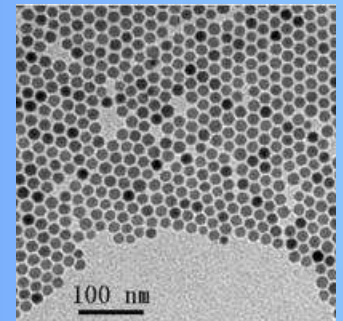
coating (variable)



Superparamagnetic NPs



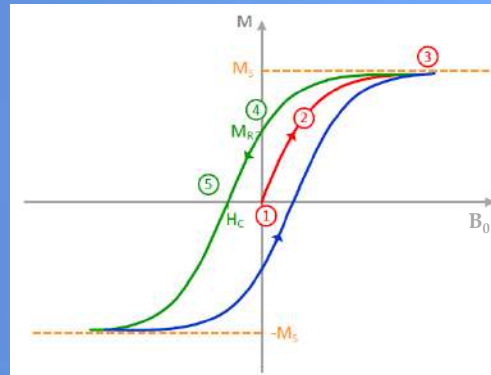
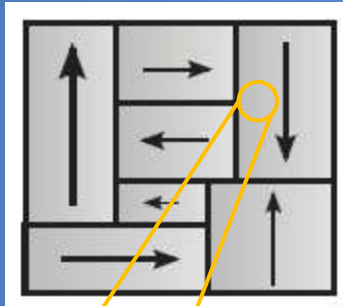
TEM



What about physico-chemical properties ?

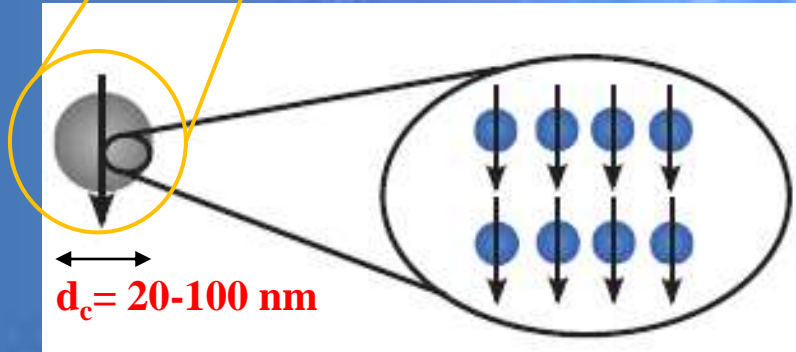
Magnetic Nanoparticles

Weiss domains

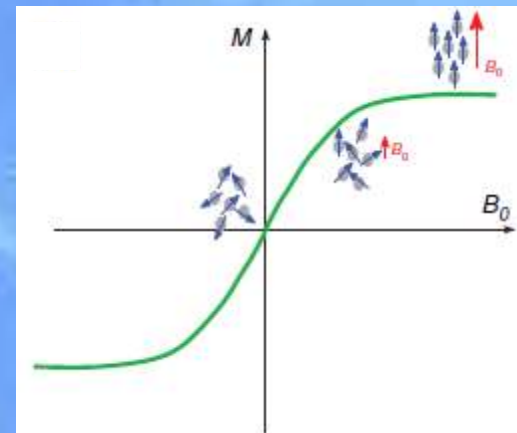
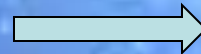


Hysteresis curve of a ferro- or ferrimagnetic material

Size effect \Rightarrow Superparamagnetism



Giant Spin



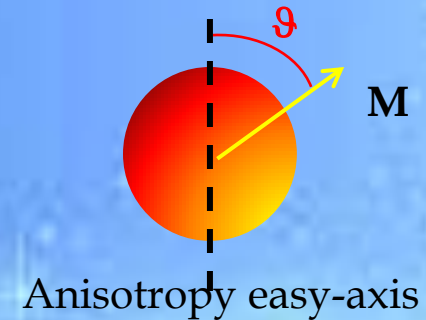
$$L(x) = \coth x - \frac{1}{x}; x = \frac{\mu_{\text{SPM}} B_0}{k_B T}$$

Small Anisotropy Energy compared to Thermal energy

Magnetic Nanoparticles

Stoner-Wolhfarth model:

The inversion of M through a **coherent movement** of all the spins of the particle

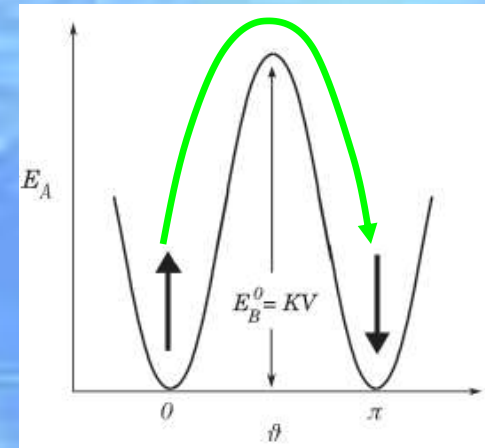


Energy barrier $E_A = k_A V \sin^2 \vartheta$

k_A = anisotropy constant, V = particle volume

$$\tau_N = \tau_0 \exp(E_A / k_B T)$$

Neel correlation time



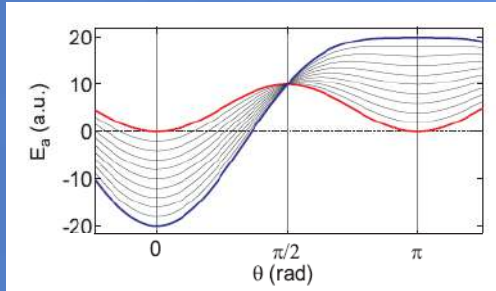
If NPs interact :

Vogel-Fulcher model, $\tau_N = \tau_0 \exp[E_A / k_B (T - T_0)]$

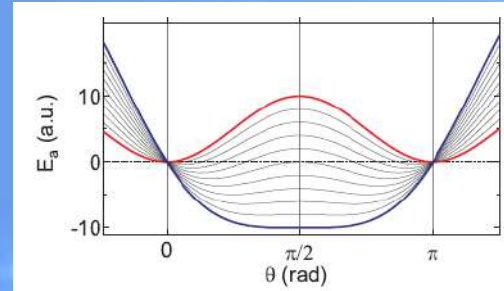
When $B_0 = 0$

Magnetic Nanoparticles

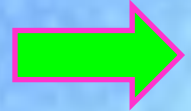
When $B_0 \neq 0$



$B_0 //$



$B_0 \perp$



But also ...

For Biomed:

MNPs dispersed in solvents

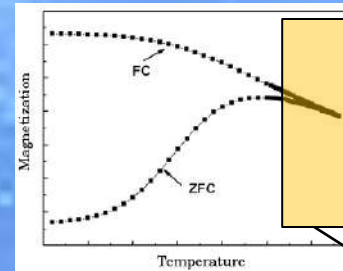
$$1/\tau = 1/\tau_N + 1/\tau_b$$

also Brownian contribution

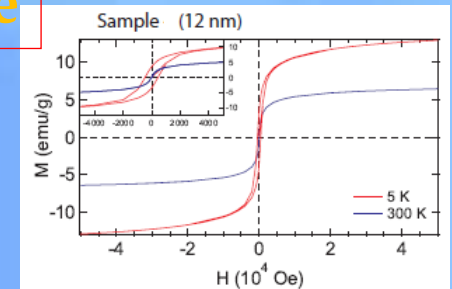
$$\tau_b = \frac{3 D_H \eta}{2 k_B T}$$

T influence

Blocking regime



Curie-Weiss

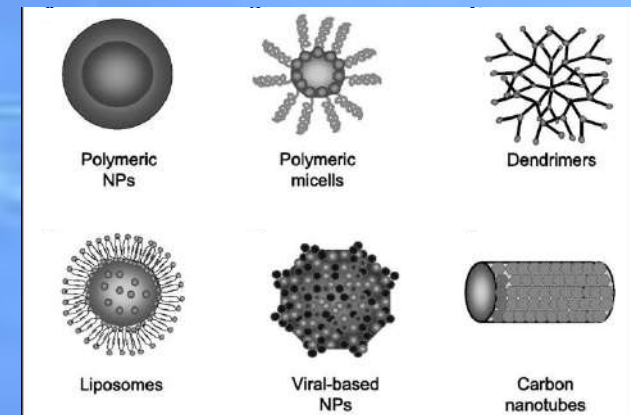
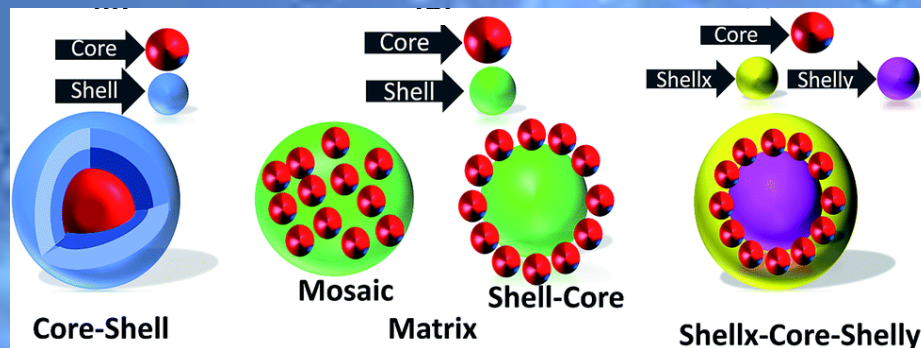
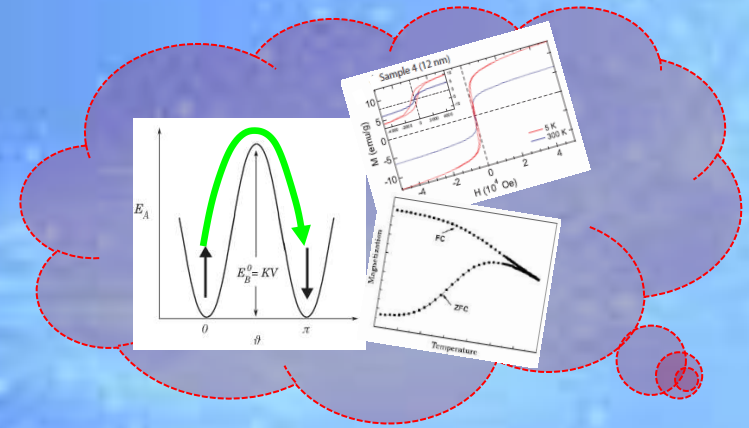


open loop

IMPORTANT: $M_{(s)}(H)$ values, magnetic anisotropy, correlation time, field and T.

Several microscopic parameters influencing the magnetic properties of superparamagnetic NPs

- Size of magnetic core
- Magnetic energy and anisotropy
- Kind of magnetic ion
- !! Kind of coating !!
- Dispersant
- Shape of the nanoparticle
- Spin Topology



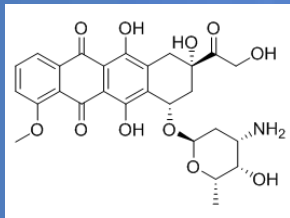
In particular... for **biomedical properties**

Kind of coating : **biocompatibility** and **targeting**

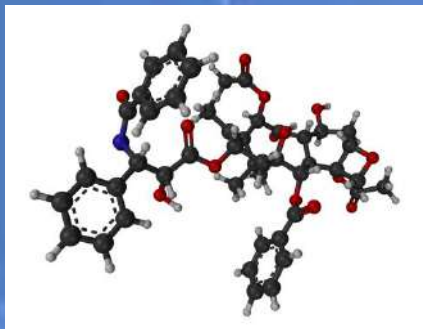
Surface **functionalization**

Fluorescent/luminescent molecules

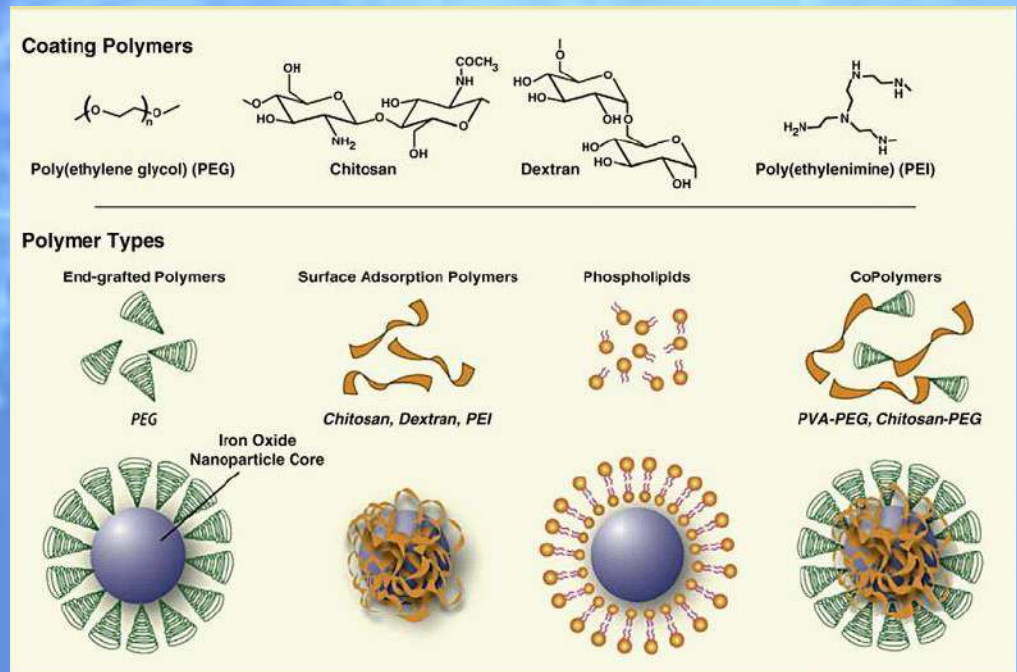
Drugs “attachment” or “inclusion”



Doxorubicine



Taxol

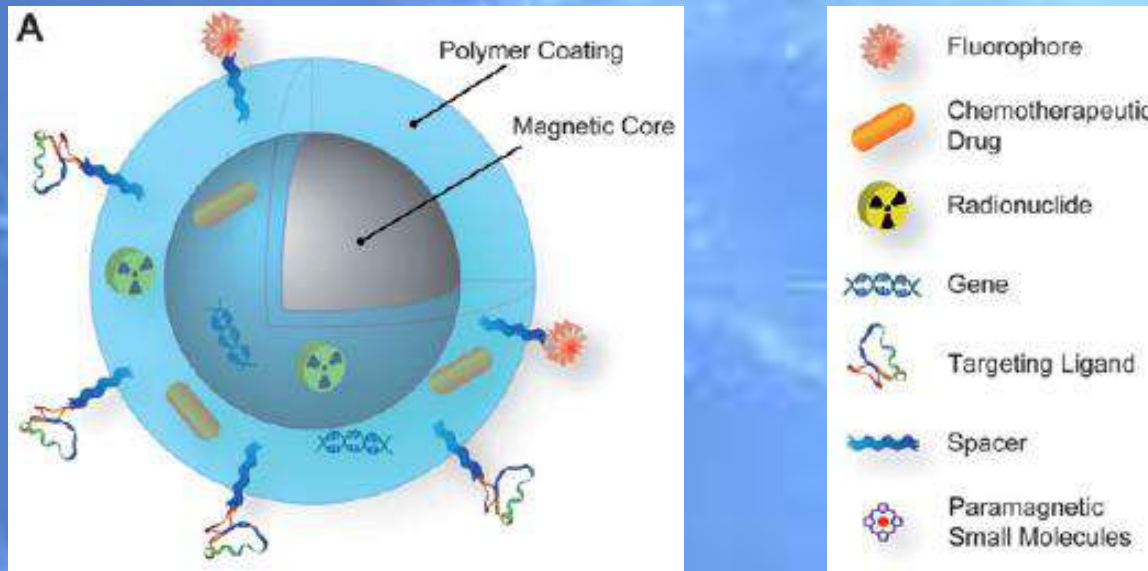


The ideal task

A single **theranostic** nano-object

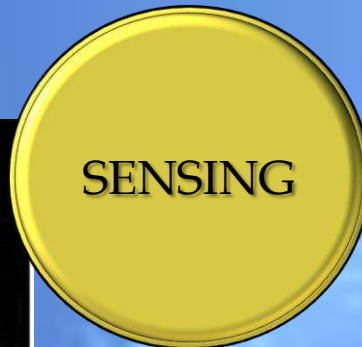
Diagnostics : MRI CA, Optical Imaging, PET, ...

Therapy : Magnetothermia (MFH), drug release



Magnetism of magnetic nanoparticles in biomedicine

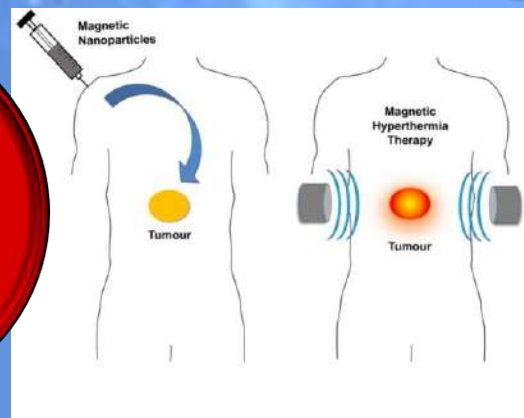
Sensing



Magnetic hyperthermia



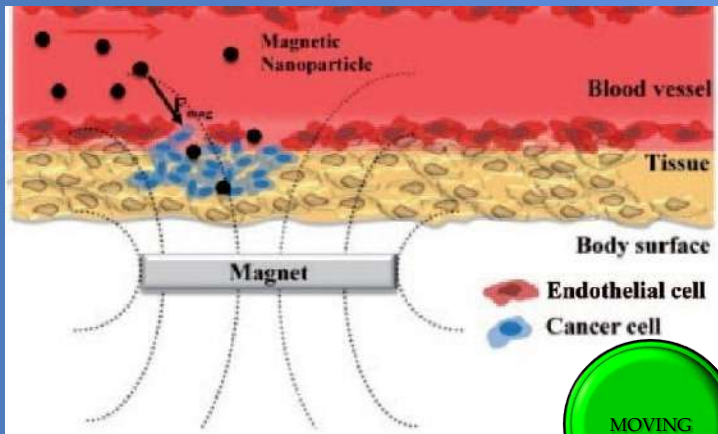
Magnetic transport



Magnetic transport (few preclinical examples)

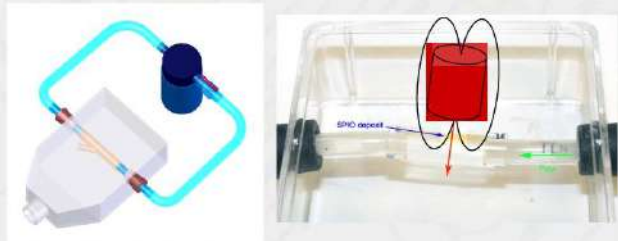
IDEA:

IV injection + local drug release
(under external stimulus)



Extravasation circulation

Prototype:



250 ml water with 5.6 mg/ml Endorem pumped at 60 ml/h for 3 h in the presence of a permanent magnet

Forces on a magnetic nanoparticle:

$$F_m = (m \cdot \nabla) B$$

$$F_m = V_m \Delta \chi \nabla (\frac{1}{2} B \cdot H)$$

Hydrodynamic drag force:

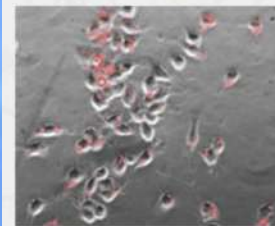
$$F_d = 6 \pi \eta R_m \Delta v$$

Equating the two:

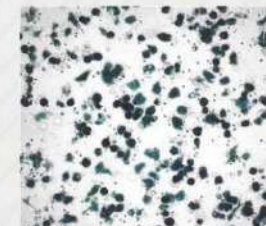
$$\Delta v = \frac{R_m^2 \Delta \chi}{9 \mu_0 \eta} \nabla (B^2) \quad \text{or} \quad \Delta v = \frac{\xi}{\mu_0} \nabla (B^2)$$

Labelling of stem cells with MNPs

Stem Cell Treatment of Atherosclerosis



In vitro labelling of Ntera2 stem cells with red fluorescent-conjugated Bangs particles

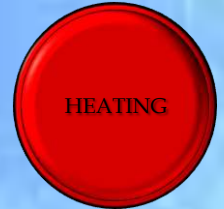


DAB-enhanced Prussian blue staining for iron following *in vitro* labelling with Endorem

... or use of magnetic field gradients for drug delivery

MFH treatment

Magnetic Fluid Hyperthermia (MFH) or Magnetothermia



Heating through application of **AC magnetic field** via activation **MNPs** directly implanted in the tumour mass at high doses (ca. 50 mg/cm^3)

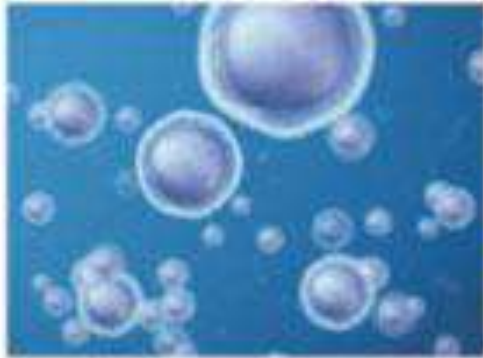
Typically in clinics: $\nu \sim 100 \text{ kHz}$, amplitude 10 kA/m

Minor side effects

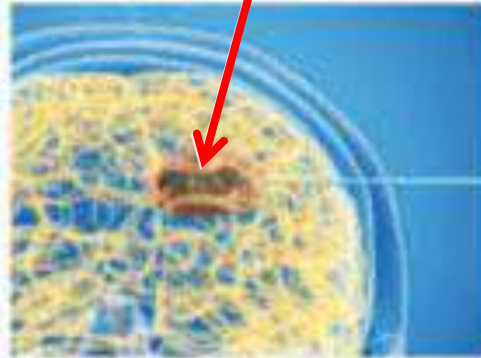
See M. Avolio and M Cobianchi posters for details

MFH: Clinical applications on Glioblastoma

MNPs coated
with amminosilane



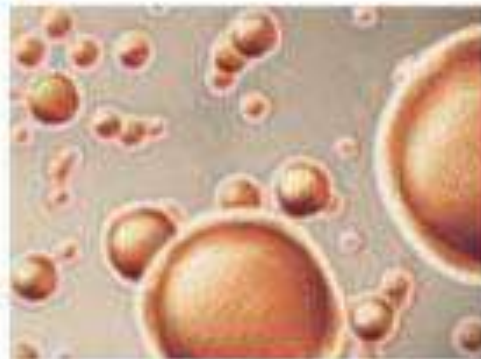
Direct injection in
the brain tumour



Tumour cells



AMF



Heating - kill tumour cells

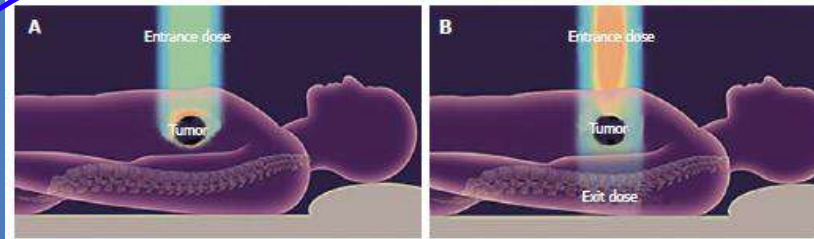


*Clinical phase II
completed*

Started a new study on glioblastoma multiforme in 2014

Several german hospitals involved

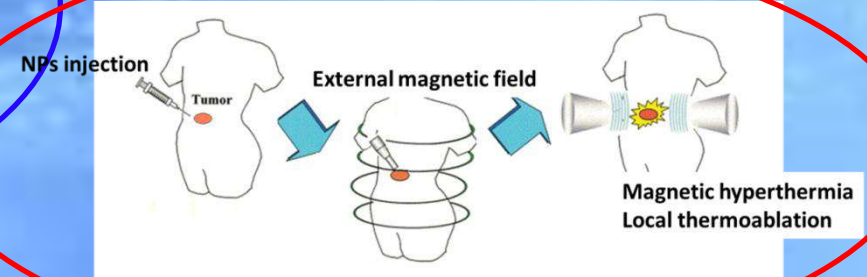
HADROCOMBI: Combining Hadron Therapy with Magnetic Hyperthermia



(A) targeted proton therapy deposits most energy on target
(B) conventional radiation therapy deposits



Illustration of MFH concept



Investigation of the **possible combined action of the two therapeutic techniques**, for going **one step beyond** the state of art of pancreatic cancer therapy. **X-rays irradiation will be used as control and comparison technique**

SENTIMAG : a sensitive susceptometer



The Sentimag® is a Class IIa device, **CE-approved for marketing and sales in Europe**, and TGA-approved for Australasia.

Sentinel lymphnodes
Technique (e.g. breast
cancer surgery)



Key features and benefits of Sienna+®:

- Particle size optimised for filtration and retention by sentinel lymph nodes
- Simple storage and handling procedure, and significantly improved workflow compared with radioactive tracers
- Localisation can start after only 20 minutes following injection†
- Natural dark brown colour eliminates the need for separate dye injections
- Non-toxic, aqueous suspension dissipates naturally in the body
- Long shelf life
- Uniquely designed and calibrated for use with Sentimag®
- Compatible with Sysmex's One-Step Nucleic Acid Amplification (OSNA) assay (<http://www.sysmex-lifescience.com/OSNA-assay-for-lymph-nodes-175-2.html>)

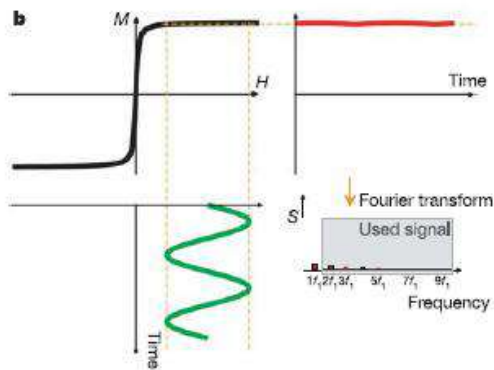
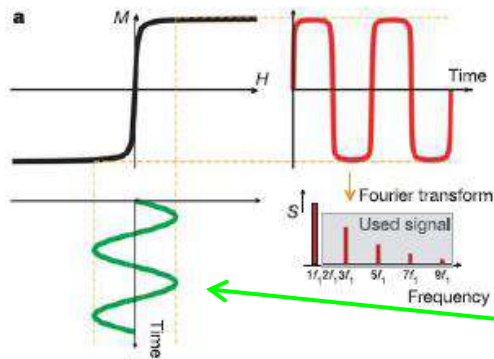
Magnetic Particle Imaging - MPI (preclinical)



It images the distribution of MNPs in biological tissues

MNPs are tracers and not just supportive contrast agents

nature
LETTERS
Tomographic imaging using the nonlinear response of magnetic particles
Bernhard Gleich^{1*} & Jürgen Weizenecker^{1,2*} Vol 435 | 30 June 2005 | doi:10.1038/nature03808



H

Oscillating field @ f_1

1st MPI system
(Bruker-Philips, 2013)



Magnetic Resonance Imaging - MRI

The most famous application of MNPs:

T₂-negative MRI contrast agents



Typical MRI apparatus for clinical use -> H = 1.5 Tesla



Prototypical example: liver tumour

without CA

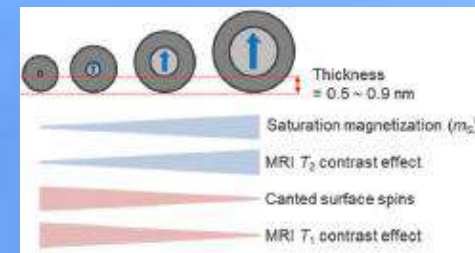


with CA



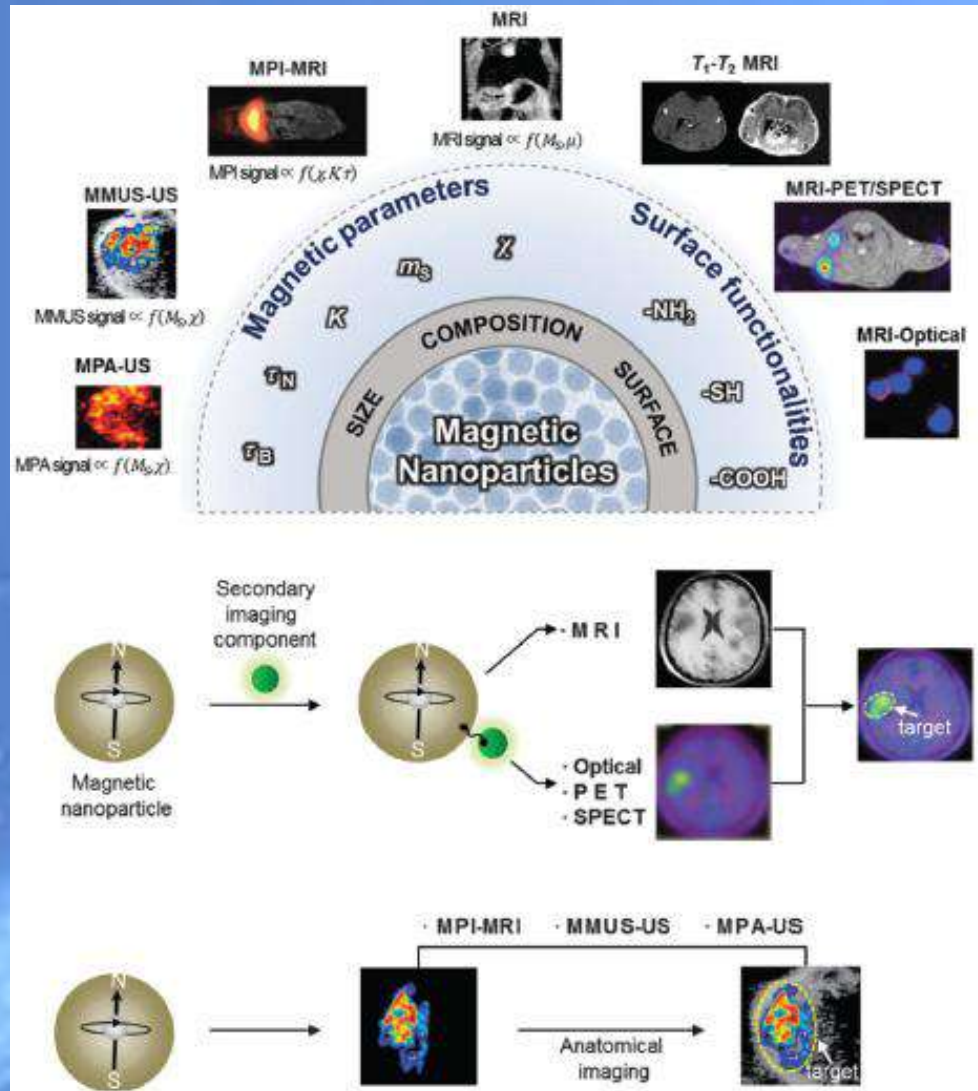
Note : MNPs also as T₁-positive agents (see e.g. Mn-ferrites)

or



... and more dual or multiple diagnostic probes. Many "lab" examples

SENSING



Most of new CA for MRI are
“non-specific” (i.e. not targeting) and so,
two crucial questions...

1) Fate of the MNPs ?

Mostly in liver if MNPs

are not reduced in total size

(and not only ...

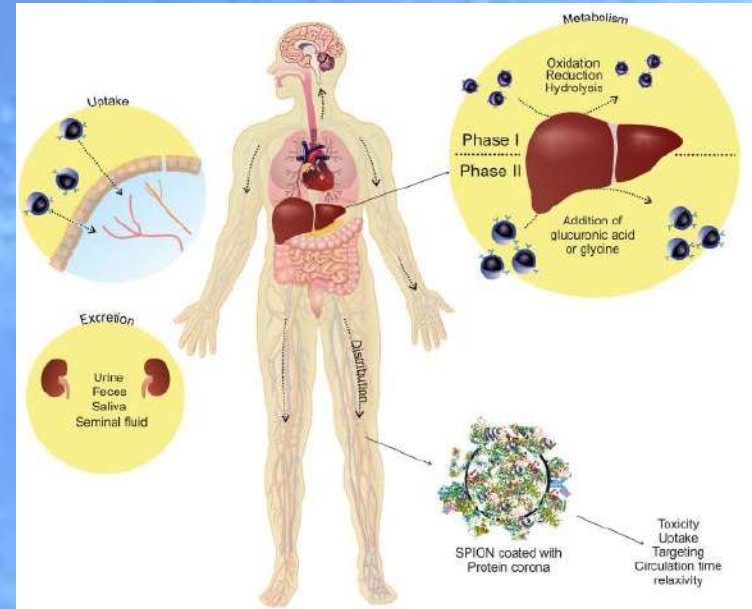
... all the physico-chemical properties

of MNPs are involved !!!)

2) Medical doctors are really interested ?

or they just point to **specific (i.e. targeting)** or

multifunctional CA ??



ALERT : SAFETY & TOXICITY !!

Focus on MRI

MRI signal is $s(t) = N(H) e^{-TE/T2} (1 - e^{-TR/T1})$

The MRI image intensity (**the contrast**) thus depends on :

Intrinsic Parameters

- Local proton density **N(H)** (water, fat)
- Nuclear Relaxation times **T₁** and **T₂**
- Magnetic susceptibility differences

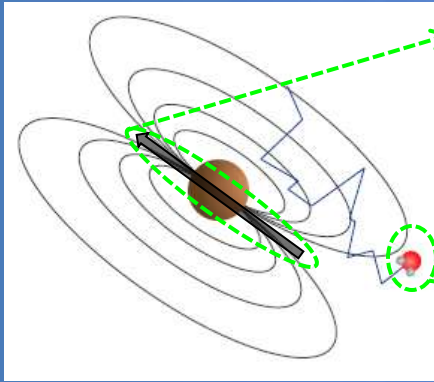
Extrinsic Parameters

- Magnetic field
- Timing of the pulse sequence
- Contrast Agents (CA)

with CA the nuclear relaxation times change
(much better idea than protons' density)

Better image contrast and pathology evidence

Focus on MRI/NMR



Fluctuations of the MNPs dipolar local field
induce

via **HYPERFINE INTERACTION**

our local probe **relaxation:**

LOCAL MAGNETIC FIELDS AND DYNAMICS can be studied with
NMR experimental parameters:

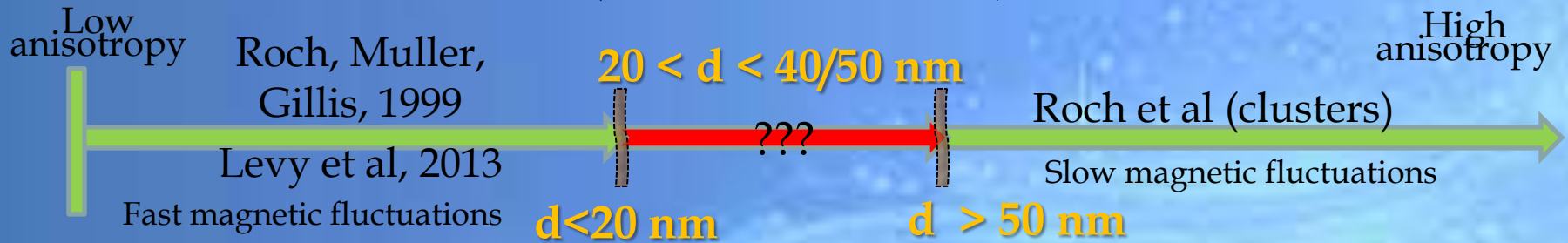
spectrum, nuclear **spin-spin** relaxation time T_2 and nuclear **spin-lattice** relaxation time T_1 $1/T_1 \propto \chi T \cdot J_e(\omega_L)$; $1/T_2 \propto \chi T \cdot J_e(0)$

and the EFFICIENCY of a CA is: $\frac{1}{T_{i,oss}} = R_{i,oss} = \frac{1}{T_{i,d}} + r_i c$

nuclear relaxivity r_i ($i=1,2$) represents the increase of nuclear relaxation rate of hydrogen nuclei in presence of 1mM of magnetic center

Focus on NMR

Mostly used models for nuclear relaxation in function of **size** (diluted SP-NPs)



Normally we consider **core $d < 20 \text{ nm}$ & spherical** shapes
(a **compromise**: good MFH efficiency and feasible targeting)

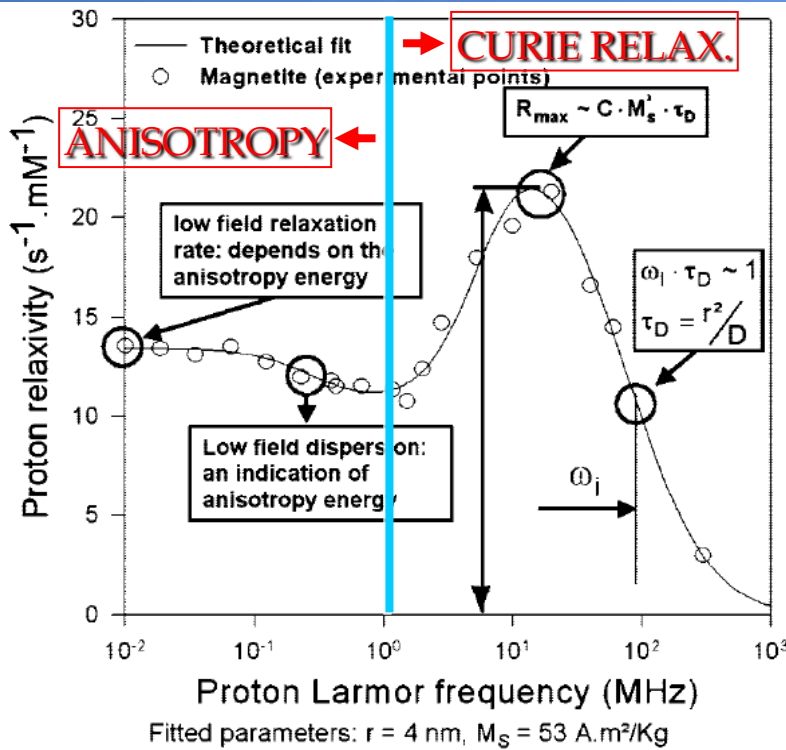
ALERT

- **Models tested for the** longitudinal nuclear relaxation rate $1/T_1$
- **We performed first** (to our kn.) **experimental complete tests** for the transverse nuclear relaxation rate $1/T_2$ (**Milano and Mons group**)
- **Simplified model for $1/T_2$** (Vuong, Gossuin, Sandre et al) -> **T_2 is the crucial parameter !!!!!!!!!!!!!!!**

Model for spherical MNPs with $d < 20\text{nm}$

(Roch, Muller, Gillis, JCP, 1999)

Typical Relaxometry curves



Analytical exact model:

$$1/T_{1,2} = f(\gamma_e, \gamma_n, \omega_L^e, \omega_L^n, \tau_{S1,2}, \tau_R, \tau_M, q, r, \tau_{S0}, \dots)$$

only for small number of spins

Heuristic "approximate" expressions

for nuclear relaxation rates

$$\begin{aligned} 1/T_1 = & (32\pi/135\,000) \mu_{SP}^2 \gamma_I^2 (N_a C / RD) \\ & \times \{ 7PL(x)/x J^F[\Omega(\omega_S, \omega_0), \tau_D, \tau_N] \\ & + [7QL(x)/x + 3(1 - L^2(x) - 2L(x)/x)] \\ & \times J^F(\omega_I, \tau_D, \tau_N) + 3L^2(x) J^A(\sqrt{2\omega_I \tau_D}) \} \end{aligned}$$

$$\begin{aligned} 1/T_2 = & (16\pi/135\,000) \mu_{SP}^2 \gamma_I^2 (N_a C / RD) \{ 13PL(x)/x J^F[\Omega(\omega_S, \omega_0), \tau_D, \tau_N] + 7QL(x)/x J^F(\omega_I, \tau_D, \tau_N) + 6QL(x)/x \\ & \times J^F(0, \tau_D, \tau_N) + [1 - L^2(x) - 2L(x)/x] [3J^F(\omega_I, \tau_D, \tau_N) + 4J^F(0, \tau_D, \tau_N)] + L^2(x) [3J^A(\sqrt{2\omega_I \tau_D}) + 4J^A(0)] \} \end{aligned}$$

Crucial : dist. min approach, magn. anisotropy, τ_N , M_s , τ_D , Langevin,

Changing the magnetic core d: r_1 heuristic fit model works

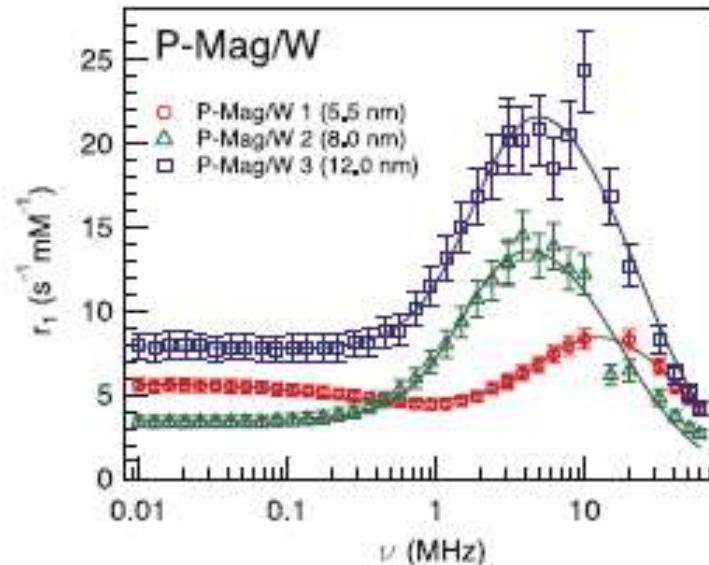
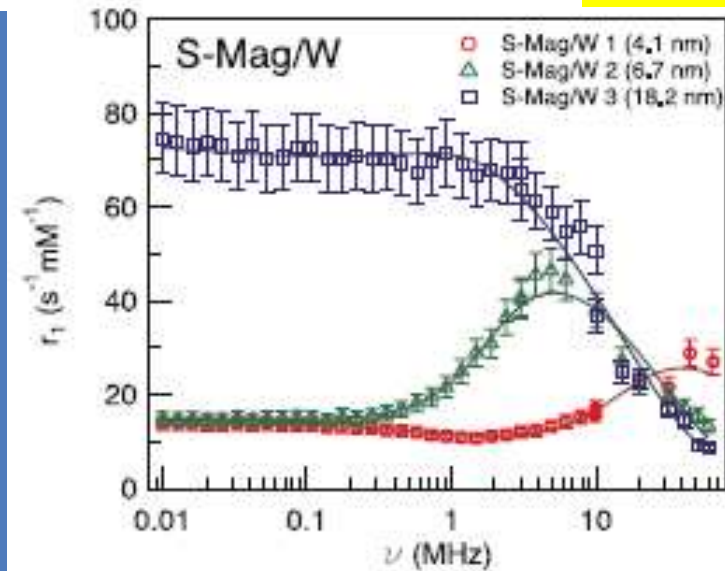
IOP Publishing
J. Phys.: Condens. Matter 25 (2013) 065901 (9pp)
doi:10.1088/0953-8948/25/06/060101

Journal of Physics: Condensed Matter
doi:10.1088/0953-8948/25/06/060101

NMR-D study of the local spin dynamics and magnetic anisotropy in different nearly monodispersed ferrite nanoparticles

L Bordonali^{1,2}, T Kalaivani^{3,4}, K P V Sabareesh^{2,3,4}, C Innocenti⁵, E Fantechi⁵, C Sangregorio^{5,6}, M F Casula⁷, L Lartigue⁸, J Larionova⁸, Y Guari⁸, M Corti^{2,4}, P Arosio^{2,3} and A Lascialfari^{2,3,4}

Fe_3O_4 magnetite 4-18 nm core, different coatings



Free parameters : r (minimum approach distance), τ_N ,
P&Q (weight of magnetic anisotropy)

COLLABORATIONS

Dept. of Chemistry and INSTM, Univ. of Firenze (Italy): C. Sangregorio (CNR), C. Innocenti, E. Fantechi, A. Caneschi, D. Gatteschi

Dept. of Chemistry and INSTM, Univ. of Cagliari (Italy): M. F. Casula, P. Floris

Montpellier University (France) Y. Guari, J. Larionova

Nantes University (France) E. Ishow, L. Lartigue

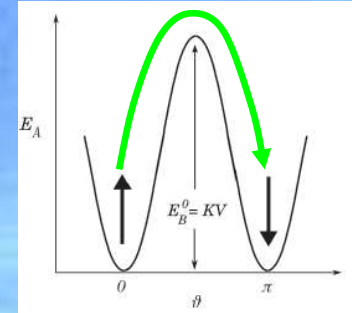
From r_1 fits one deduces mainly

* Regarding **magnetization reversal** :

“local” τ_0 and anisotropy barrier E_A , i.e. info about

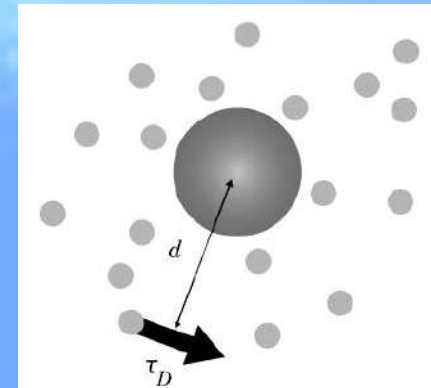
“local” Neel correlation time τ_N

(comparison with χ_{AC} \rightarrow bulk)



* The **distance of minimum approach**. This is influenced by coating/functionalization of the sample, and often “ignored” in models.

Comparison with AFM, DLS and TEM data.

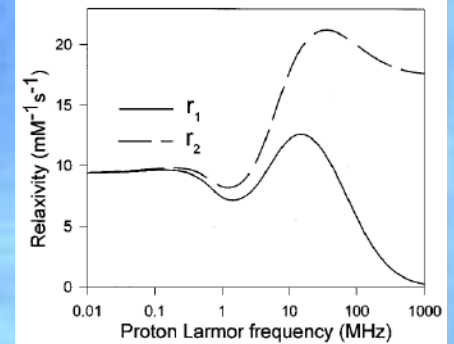


* Information on **magnetic anisotropy**.

Changing the magnetic core: r_1 ok, but r_2 ...

First complete experimental r_2 -relaxivity profile

Theoretical NMR-D curves



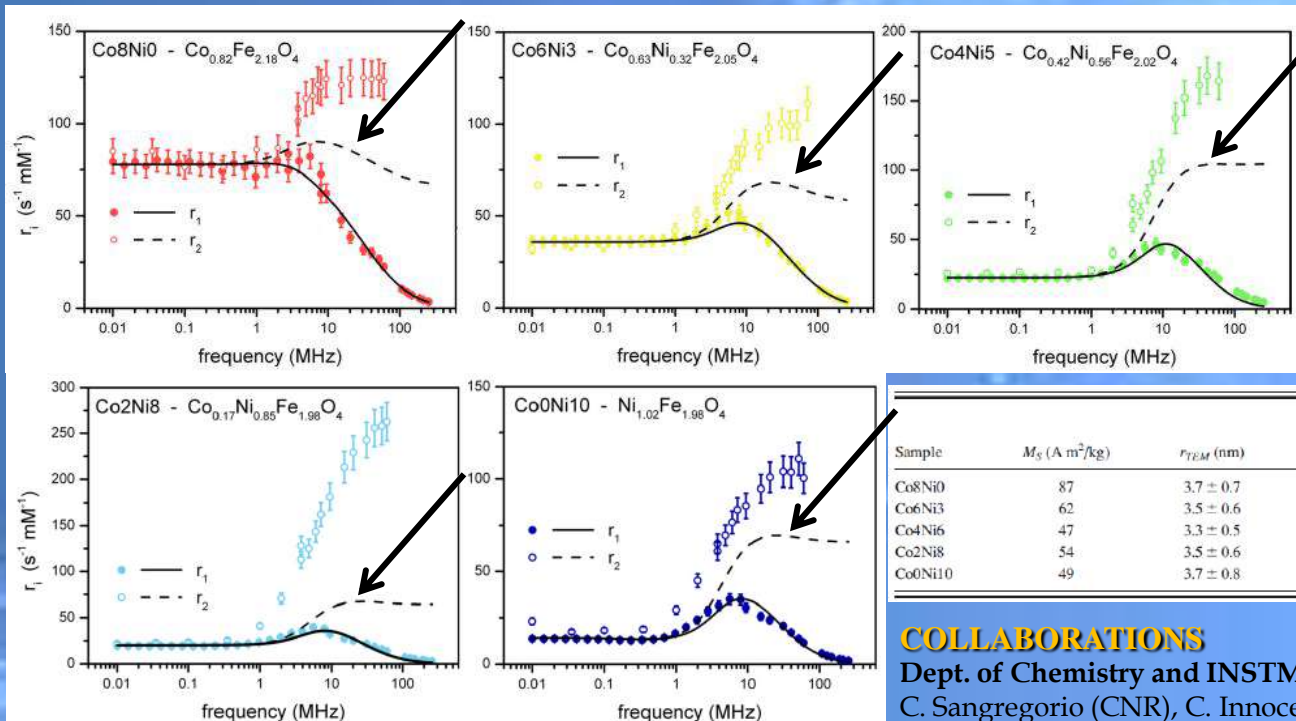
JOURNAL OF APPLIED PHYSICS **119**, 134301 (2016)

On the magnetic anisotropy and nuclear relaxivity effects of Co and Ni doping in iron oxide nanoparticles

T. Orlando,^{1,2,a)} M. Albino,³ F. Orsini,⁴ C. Innocenti,³ M. Basini,^{4,5} P. Arosio,⁴ C. Sangregorio,^{3,6} M. Corti,¹ and A. Lascialfari^{4,5}

Sample	Composition
Co8Ni0	Co _{0.82} Fe _{2.18} O ₄
Co6Ni3	Co _{0.63} Ni _{0.32} Fe _{2.05} O ₄
Co4Ni5	Co _{0.42} Ni _{0.56} Fe _{2.02} O ₄
Co2Ni8	Co _{0.17} Ni _{0.85} Fe _{1.98} O ₄
Co0Ni10	Ni _{1.02} Fe _{1.96} O ₄

SAME FIT Dashed = r_2
PARAMETERS Solid = r_1



Sample	M_s (A m ² /kg)	r_{TEM} (nm)	r_{AFM} (nm)	NMR fitting parameters			P
				r_{NMR} (nm)	r_d (nm)	τ_N^{NMR} (s)	
Co8Ni0	87	3.7 ± 0.7	4.0 – 6.9	4.3(1.7)	5.0(0.1)	4.7(1.2) × 10 ⁻⁸	0
Co6Ni3	62	3.5 ± 0.6	4.0 – 6.9	4.0(0.2)	4.8(0.1)	4.9(0.3) × 10 ⁻⁹	0
Co4Ni5	47	3.3 ± 0.5	4.3 – 7.3	4.0(0.2)	6.9(0.4)	1.7(0.2) × 10 ⁻⁹	0
Co2Ni8	54	3.5 ± 0.6	4.4 – 7.5	4.1(0.1)	6.8(0.4)	2.9(0.3) × 10 ⁻⁹	0
Co0Ni10	49	3.7 ± 0.8	4.2 – 6.9	4.5(0.2)	6.9(0.4)	1.7(0.2) × 10 ⁻⁹	0.15

COLLABORATIONS

Dept. of Chemistry and INSTM, Univ. of Firenze (Italy):

C. Sangregorio (CNR), C. Innocenti, E. Fantechi, A. Caneschi, D. Gatteschi

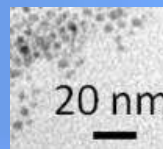
Dept. of Physics and INSTM, Univ. of Pavia (Italy): M. Corti

... maghemite, model for r_2 does not work again

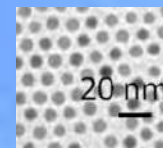
THE JOURNAL OF CHEMICAL PHYSICS 146, 034703 (2017)

Local spin dynamics of iron oxide magnetic nanoparticles dispersed in different solvents with variable size and shape: A ^1H NMR study

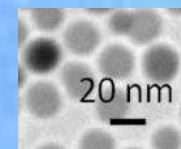
M. Basini,¹ T. Orlando,² P. Arosio,¹ M. F. Casula,³ D. Espa,³ S. Murgla,³ C. Sangregorio,⁴ C. Innocenti,⁵ and A. Lascialfari^{1,6}



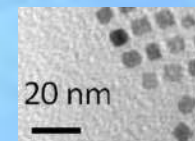
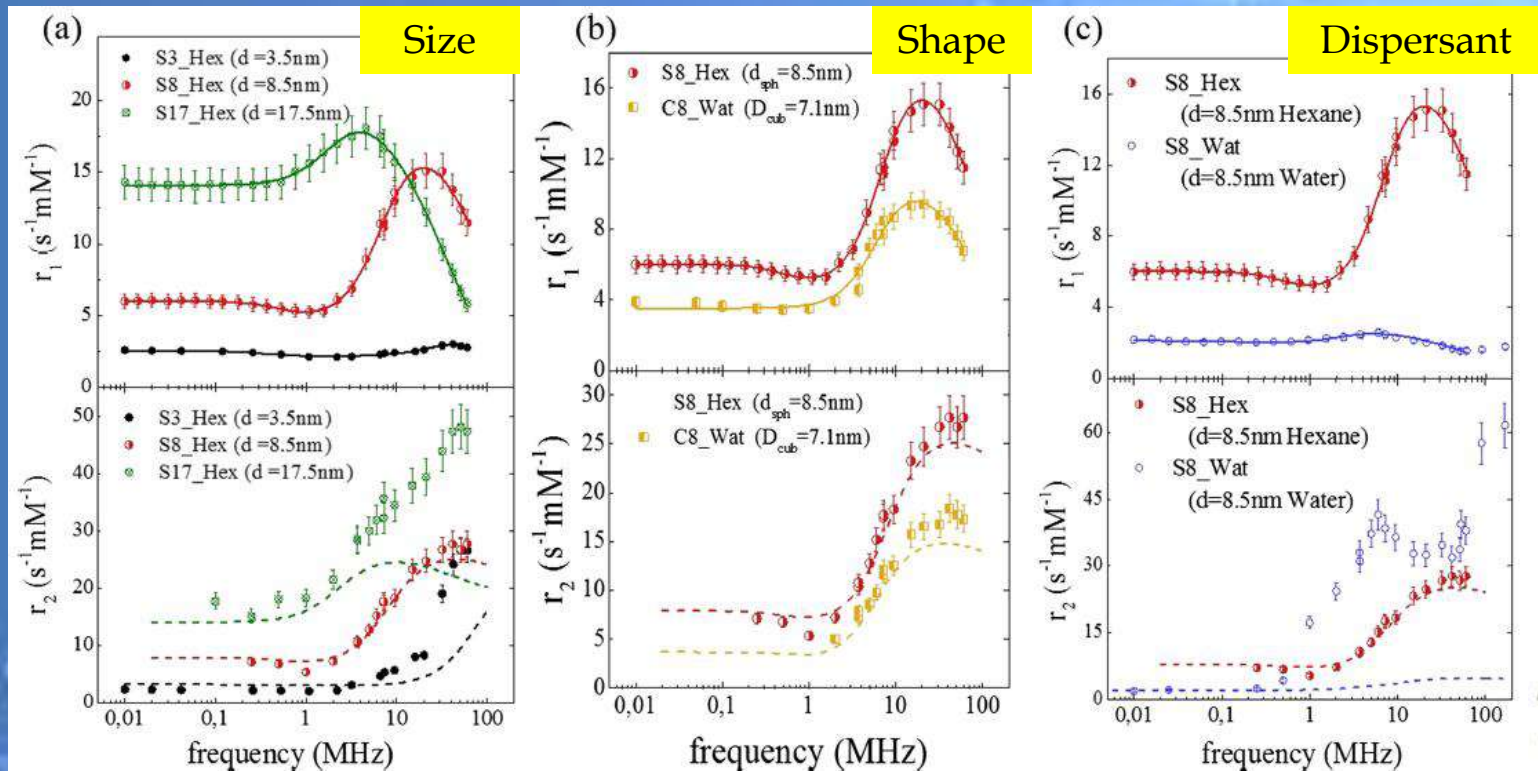
S3_Hex



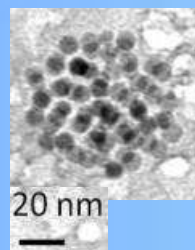
S8_Hex



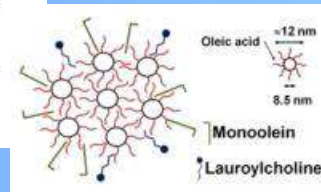
S17_Hex



C8_Hex



S8_Wat



COLLABORATIONS

Dept. of Chemistry and INSTM, Univ. of Firenze (Italy): C. Sangregorio (CNR), C. Innocenti, E. Fantechi, A. Caneschi, D. Gatteschi

Dept. of Chemistry and INSTM, Univ. of Cagliari, Cagliari (Italy): M. F. Casula, P. Floris

A really simplified model for T_2

Simplifying the heuristic expression:

A Universal Scaling Law to Predict the Efficiency of Magnetic Nanoparticles as MRI T2-Contrast Agents

Quoc L. Vuong, Jean-François Berret, Jérôme Fresnais, Yves Gossuin,* and Olivier Sandre*

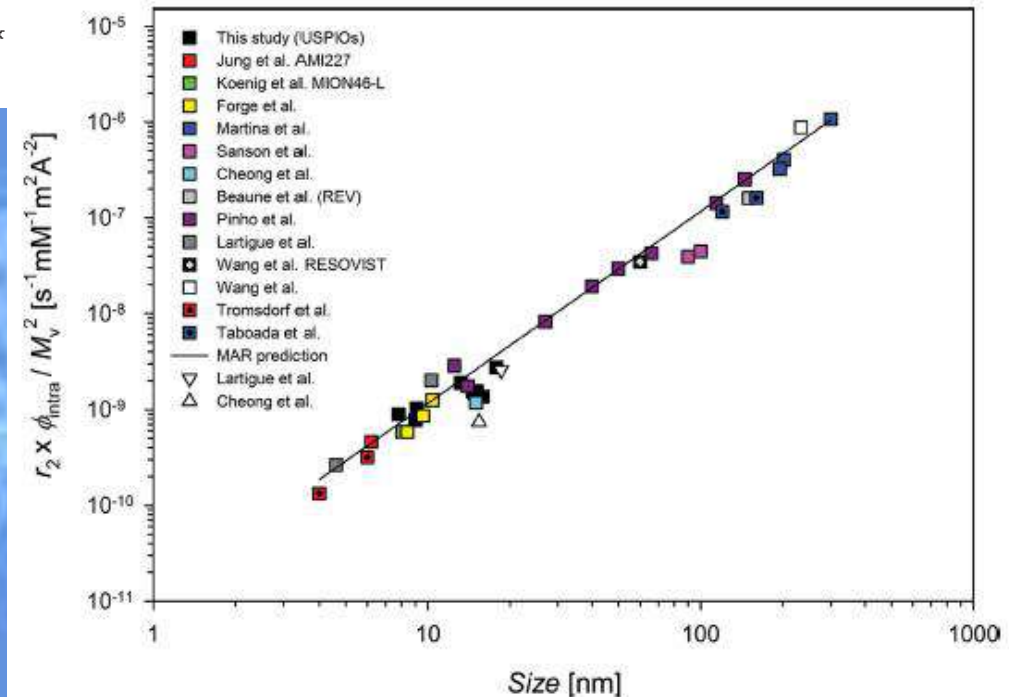
Adv. Healthcare Mater. 2012,
DOI: 10.1002/adhm.201200078

$$r_2 = \frac{R_2}{[\text{Fe}]} = \frac{4\gamma^2 \mu_0^2 \nu_{\text{nat}} M_V^2 d^{22}}{405 D}$$

which is valid only if the Redfield condition is fulfilled:

$$\Delta\omega_{\text{HD}} < 1 \quad \text{MAR}$$

$$r_2^* = \frac{R_2^*}{[\text{Fe}]} = \frac{2\pi \gamma \mu_0 \nu_{\text{nat}} M_V}{9\sqrt{3}} \approx r_2 \quad \text{SDR}$$



But for a complete theory a more refined model is needed !

Study in progress..... influence of interparticle interactions, microaggregation, water (exchange-penetration & coating interaction with bulk) role, Brownian motion (if...),.....

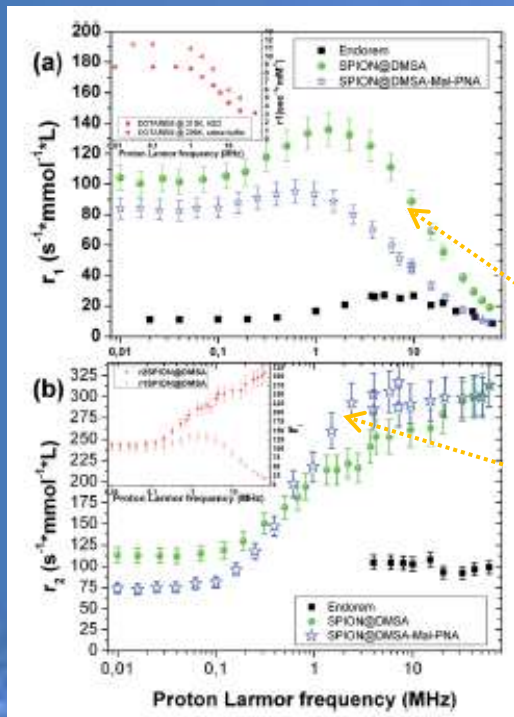
Other cases

Functionalization effect

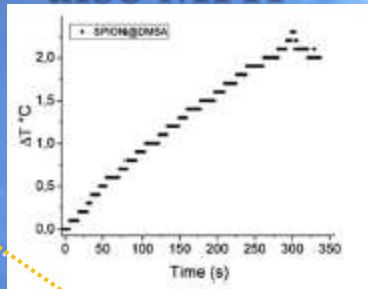
RSC Advances Cite this: *RSC Adv.*, 2017, 7, 15500

Superparamagnetic iron oxide nanoparticles functionalized by peptide nucleic acids†

Marco Galli,^a Andrea Guerrini,^b Silvia Cauteruccio,^a Pramod Thakare,^a Davide Dova,^a Francesco Orsini,^c Paolo Arosio,^c Claudio Carrara,^a Claudio Sangregorio,^{de} Alessandro Lascialfari,^{ce} Daniela Maggioni^{ae} and Emanuela Licandro^{ae}

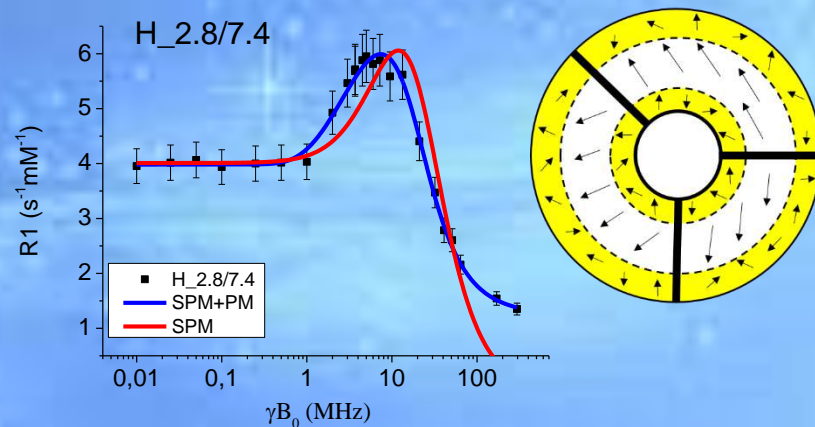
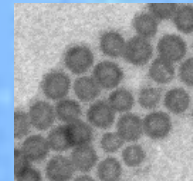


also MFH



changes of r_i

Hollow topology Surface vs bulk Spins



$$\frac{1}{T_1} = A'_{\%} HF \frac{\tau_c}{(1 + \omega^2 \tau_c^2)} + (1 - A'_{\%}) \frac{1}{T_1^{Heu}}$$

$$\frac{1}{\tau_c} = \frac{1}{\tau_{SI,PM}} + \frac{1}{\tau_D}$$

$$\tau_{SI,PM} = \tau_0 e^{\frac{E_B^{surf}(ZFC)}{k_B T}}$$

$$\tau_D = \frac{r^2}{D}$$

paramagnetic contribution

(also other evidences: magnetic, MuSR, ...)

See M. Basini poster

COLLABORATIONS

Dept. of Chemistry and INSTM, Univ. of Milano :
G. D'Alfonso, D. Maggioni, E. Licandro, et al

COLLABORATIONS

ISM-CNR, Roma: D. Peddis, et al

MR images about targeting: towards molecular imaging

Within EU- FP7-Nanother

RSC Advances

PAPER



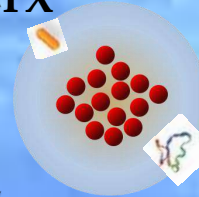
Cite this: RSC Adv., 2015, 5, 39760

MR imaging and targeting of human breast cancer cells with folate decorated nanoparticles†

Paolo Arosio,^a Francesco Orsini,^a Anna M. Piras,^b Stefania Sandreschi,^b Federica Chiellini,^b Maurizio Corti,^c Marc Masa,^d Marta Múčková,^e Ludmila Schmidová,^e Costanza Ravagli,^f Giovanni Baldi,^f Elena Nicolato,^g Giamaica Conti,^g Pasquina Marzola^h and Alessandro Lascialfari^a

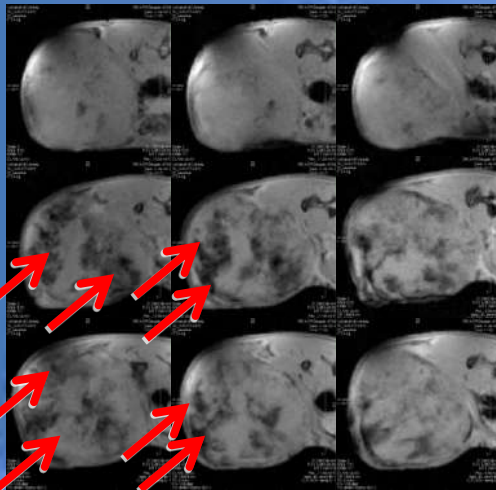
- * MDA-MB-231 human breast cancer
- * Subcutaneous implantation

PTX



Folate

GE T2*W

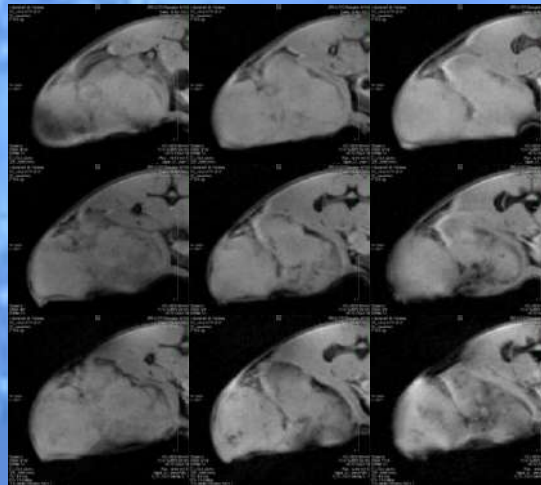


PRE

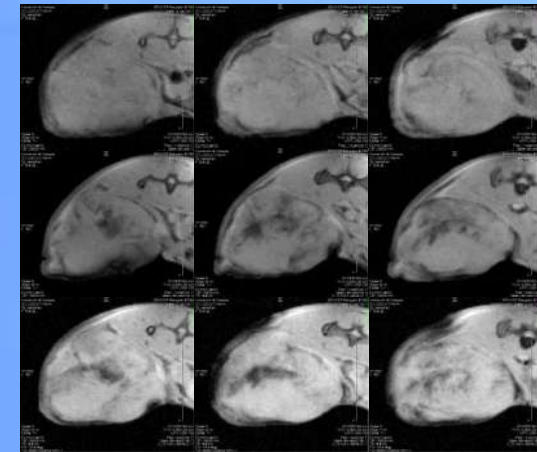
POST

POST 24 H

NPs with folic acid



NPs without folic acid



Endorem

Conclusions (not exhaustive)

- * Nowadays For ferrites **$d > 10 \text{ nm}$** is ok (well joint to $d > 14 \text{ nm}$ for MFH), but **the size** is crucial for bio-application -> **reducible?**
- * **Surface spins/Solvent/ Coating** effects to be clarified
- * Role of **interparticle interactions**? Theoretically manageable ?
- * Need for **specific model if functionalization** with drugs, fluo molecules, antibodies/peptides, are implemented
- * Industrial scalability (stimulate companies interest)
- * **Control** Protein Corona effect and **avoid (except specific cases)** macrophages actions
- * **Poor specific uptake** in tumor tissue **proved. Percentage** enough for?
- * Cells mechanism of uptake and EPR (Enhanced Permeability and Retention) effect
- * Problems of **haemagglutination** and **aggregation**
- * **Toxicity** has to be established case by case

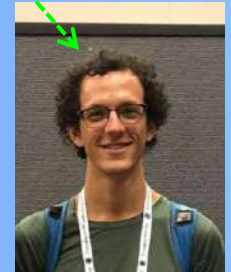
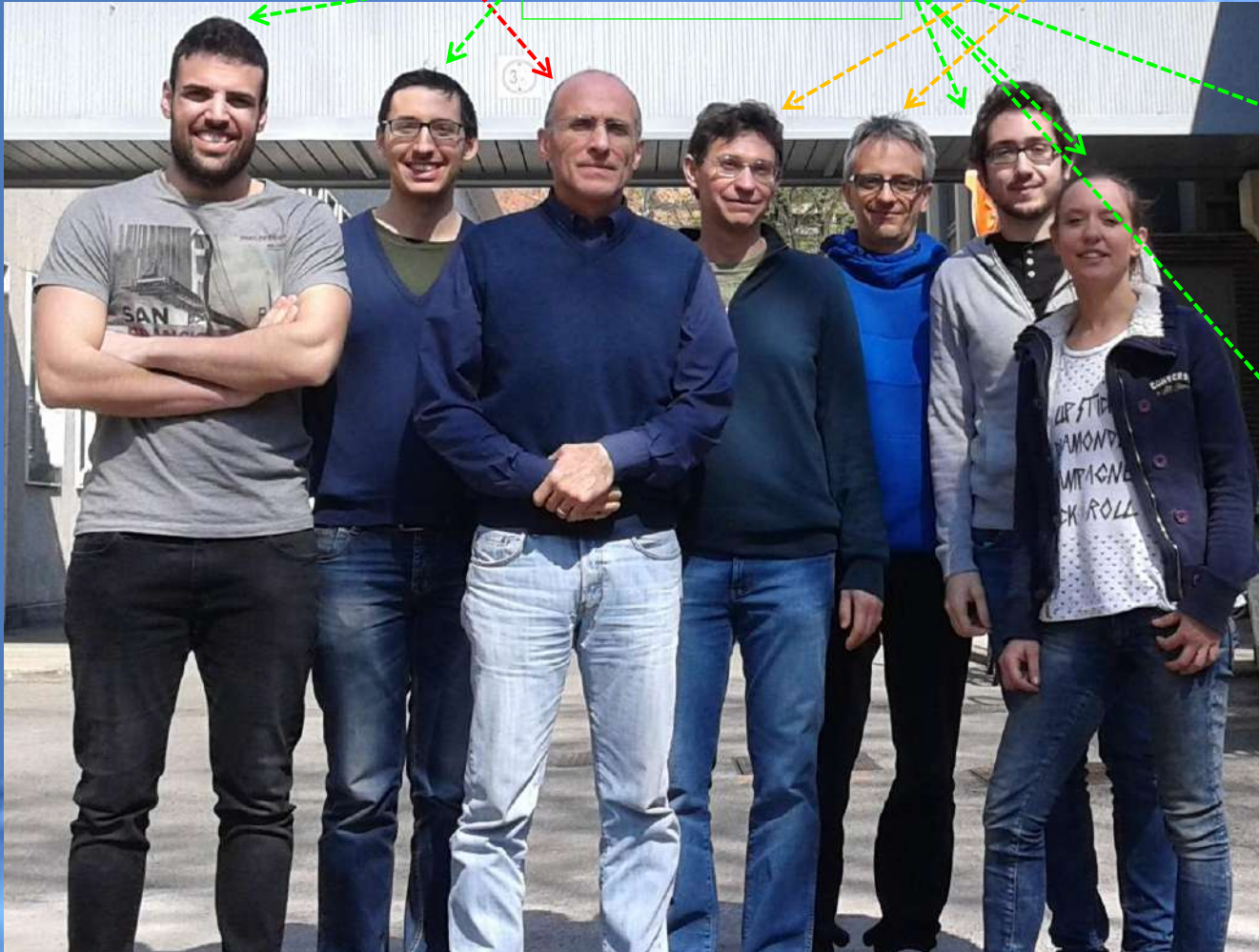
Crucial passage for new systems is from in-vitro to in-vivo !!!

Our Group

The boss

The old pillars

The workers







Comparison of different kinds of Hyperthermia

Heating by microwave and radiofrequency sources

- good localization at shallow depths
- **Weaknesses** : (i) cannot become selective; (ii) high temperature also all around in normal tissues; (iii) at greater tumor depths, even with lowered frequency, the localization is much poorer; (iv) invasivity of the implant; (v) many repeated treatments (thermo-tolerance)

Heating by ultrasound sources (and HiFUS)

- good penetration and temperature can be achieved in soft tissues
- **Weaknesses** : (i) cannot become selective; (ii) high temperature also all around in normal tissues (MRI confirms); (iii) the presence of bone or air cavities causes distortions of the heating pattern; (iv) many repeated treatments (thermo-tolerance)

Magnetic Fluid Hyperthermia

- **Advantages of MFH** : (i) Innovation : joint to Hadron-therapy first time (in literature, in combination just with radiotherapy); (ii) local temperature increase/control, normal tissues negligibly affected; (iii) no implant invasivity; (iv) less theoretical limitation vs kind of tumour; (v) single injection also for repeated treatments; (vi) tumor reachable at greater depth; (vii) in perspective the magnetic nanoparticles can carry a drug or antibodies, peptides, etc. (MFH can become selective)
- **Weaknesses** : high MNPs doses (from literature no short/medium-term major side effects), inhomogeneity of MNPs spatial distribution

Specific Absorption Rate (SAR)

SAR: the **rate** at which **energy** is **adsorbed** by the body when exposed to a **radio frequency** (RF) **electromagnetic field** (generally 100 kHz ÷ 1 GHz).

It is also called SLP (Spcific Loss Power)

It is defined as the **power** absorbed per **mass** of **tissue** (W/kg).

SAR can be calculated from the electric field or the magnetic field within the tissue as:

$$\text{SAR} = \int_{\text{sample}} \frac{\sigma(\mathbf{r}) |\mathbf{E}(\mathbf{r})|^2}{\rho(\mathbf{r})} d\mathbf{r}$$

$$P_{FM} = \mu_0 f \oint H dM$$

$$(\text{SAR} \equiv P_{FM})$$

where σ is the sample **electrical conductivity**, E is the **RMS** electric field, H the **RMS** magnetic field, f the **frequency** of H , M the **magnetization**, ρ is the sample **density**

In **magnetic hyperthermia** is expressed in W/g of nanoparticles:

(i) $\text{SAR} = A \cdot f$ (hysteresis losses) or (ii)

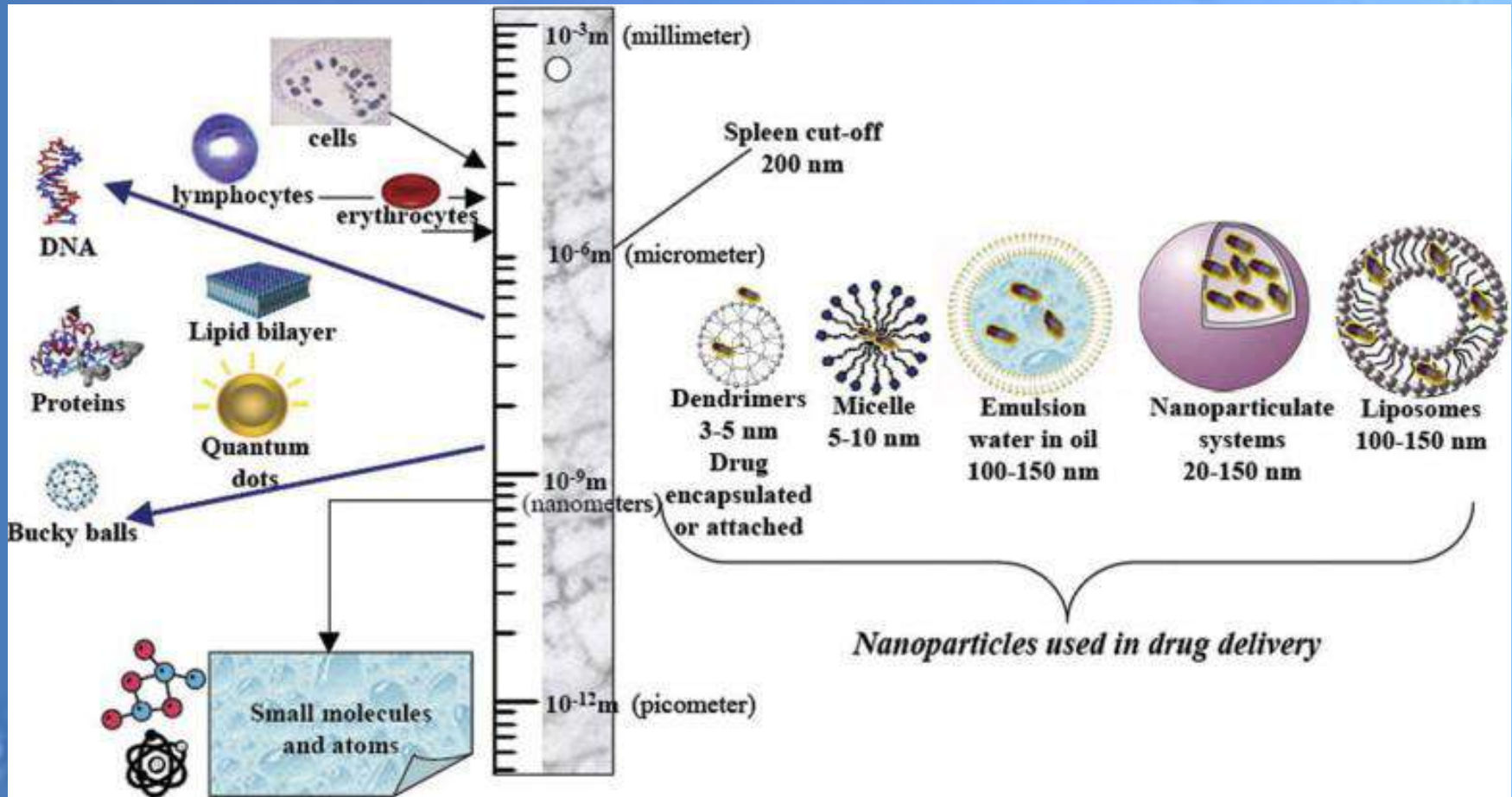
(ii) $\text{SAR} \propto f \chi''(t) H_0^2$ (relaxation losses, **Brownian/Neel**)

where A = area of the hysteresis loop and f = frequency of the *rf* magnetic field.

In the case of MNP, **A** depends on K, V, T, f, H_0, c

Coming back to the origin

Typical dimensions in biomedicine



Why MRI ?

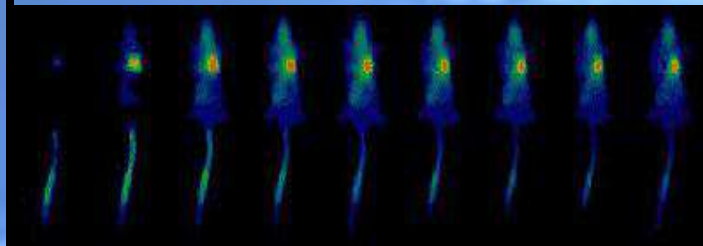
Nuclear Medicine:

- Poor spatial resolution
- Poor temporal resolution
- High sensitivity
- Reporters: radionuclides



Optical Imaging:

- Poor spatial resolution
- Poor temporal resolution
- high sensitivity
- Reporters: luminescent probes



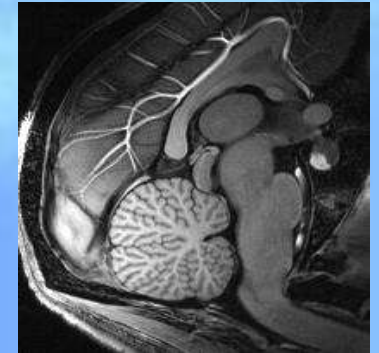
X-Ray (CT):

- Good spatial resolution
- Good temporal resolution
- Low sensitivity



MRI:

- **Non-invasive**
- Good spatial resolution
- Good temporal resolution
- Low sensitivity



For biomed: our roles let us to

-Help the chemists

Accurate study of Chemico-Physical properties of MNPs ->
choice of better **synthetic pathways** to follow

- Understand the hopeful application

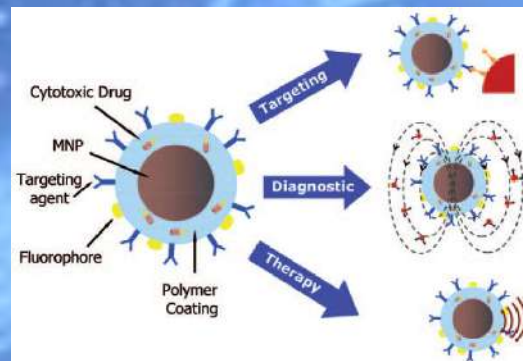
Diagnostics

CAs

Therapeutics

Hyperthermia/ drug delivery

... again



If "tumour (disease) targeting" at the level of clinical applications is actually almost **prohibitive**,
what could be the "industry" and clinicians interests ?

Still obtaining a "**small**" non-specific CA,
with well controllable synthesis and
with **efficiency** (relaxivity) **higher** than
actual ones (**lower costs, lower doses**)
BUT SAFE !

This "guides" the **research** about controlling the
physical mechanisms/parameters
that enhances the nuclear relaxation

Examples of other models for SP MNPs

THE JOURNAL OF
PHYSICAL CHEMISTRY C

Revisiting MRI Contrast Properties of Nanoparticles: Beyond the Superparamagnetic Regime

Michael Levy, Florence Gazeau, Claire Wilhelm, Sophie Neveu, Martin Devaud, and Pierre Levitz

J. Phys. Chem. C, Just Accepted Manuscript • DOI: 10.1021/jp404199f • Publication Date (Web): 25 Jun 2013

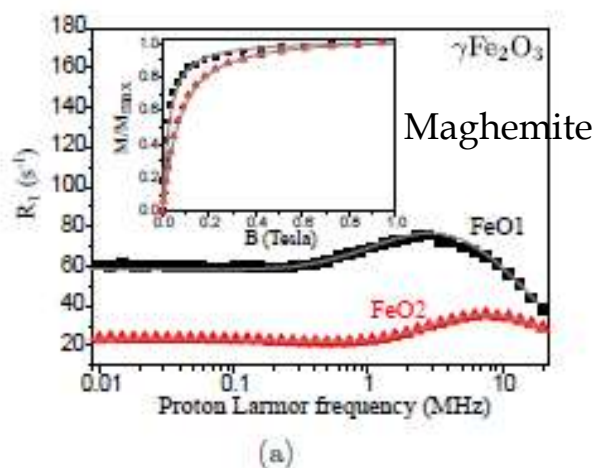
Downloaded from <http://pubs.acs.org> on July 3, 2013

Journal of Magnetism and Magnetic Materials 293 (2005) 532–539

Superparamagnetic colloid suspensions: Water magnetic relaxation and clustering

Alain Roch^a, Yves Gossuin^b, Robert N. Muller^a, Pierre Gillis^{b,*}

Clusters (theory)



Co-ferrite

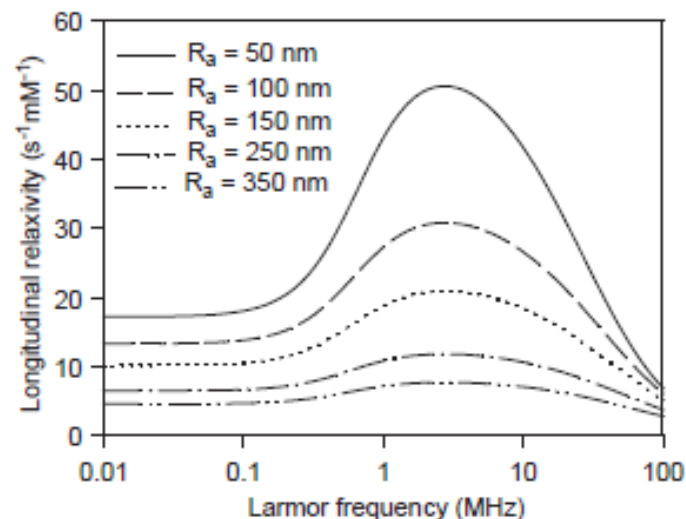
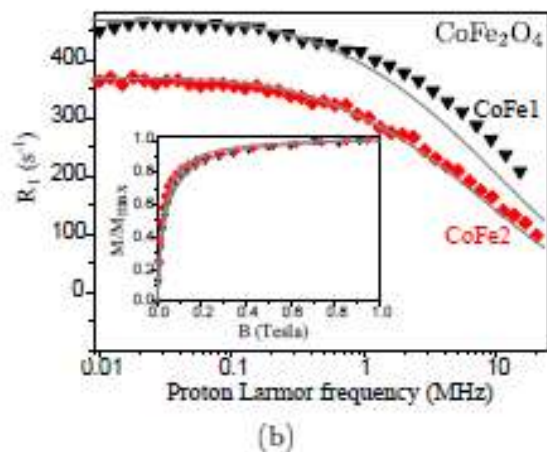


Fig. 2. Theoretical longitudinal NMRD profiles from Eq. (14). The parameters characterizing the elementary grains are given in the text.

Figure 1: Experimental NMRD profiles and theoretical fits (solid lines) of suspensions of (a) $\gamma\text{Fe}_2\text{O}_3$ and (b) CoFe_2O_4 NPs (iron concentration $[\text{Fe}] = 1 \text{ mM}$). The fits are obtained as explained in the text using $T = 298 \text{ K}$, $\eta = 0.89 \times 10^{-3} \text{ Pa}\cdot\text{s}$ and M_s the bulk value ($412 \text{ kA}\cdot\text{m}^{-1}$ for $\gamma\text{Fe}_2\text{O}_3$ and $398 \text{ kA}\cdot\text{m}^{-1}$ for CoFe_2O_4). The adjustable parameters used for each sample are the following. For FeO1: $K=9000 \text{ J}\cdot\text{m}^{-3}$, $\tau_0 = 6 \times 10^{-8} \text{ s}$, $\alpha = 0.11$ and $\delta = 1.8 \text{ nm}$. For FeO2: $K=6000 \text{ J}\cdot\text{m}^{-3}$, $\tau_0 = 5 \times 10^{-9} \text{ s}$, $\alpha = 0.19$ and $\delta = 1.4 \text{ nm}$. For CoFe1: $\delta = 1.5 \text{ nm}$. For CoFe2: $\delta = 0.5 \text{ nm}$. Insets show the normalized magnetization curves fitted with polydisperse Langevin functions (solid lines) to determine the characteristic diameter d_0 and polydispersity σ_0 of the NP log-normal size distributions. We found: for FeO1: $d_0 = 9.2 \text{ nm}$, $\sigma_0 = 0.22$; for FeO2: $d_0 = 7 \text{ nm}$, $\sigma_0 = 0.2$; for CoFe1: $d_0 = 7.9 \text{ nm}$, $\sigma_0 = 0.32$ and for CoFe2: $d_0 = 6.2 \text{ nm}$, $\sigma_0 = 0.4$.

Clinical Note

Ferumoxytol in Clinical Practice: Implications for MRI

Brendan J. McCullough, MD, PhD,* Orpheus Kolokythas, MD, Jeffrey H. Maki, MD, PhD, and Douglas E. Green, MD

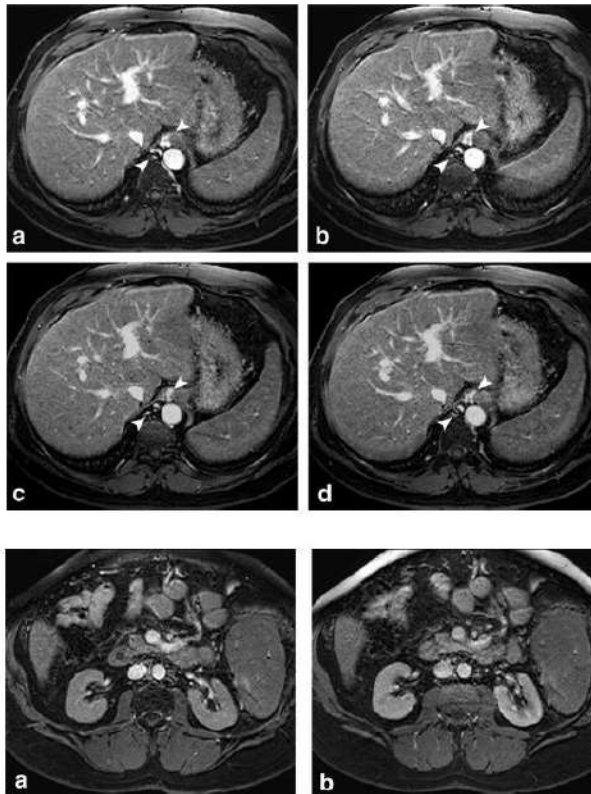


Figure 1. T1 shortening from ferumoxytol results in blood pool hyperintensity, obscuring enhancement from GBCA. Axial T1-weighted image prior to GBCA administration (a) and post-contrast images during arterial (b), portal venous (c), and equilibrium phases (d) show unchanged enhancement. Note is made of small esophageal varices (arrowheads).

Figure 2. Renal cortical enhancement confirms appropriate administration of GBCA. Axial T1-weighted image demonstrates homogenous signal intensity of the kidneys before administration of GBCA (a). Following injection of GBCA (arterial phase), there is perceptible enhancement of the renal cortex (b).

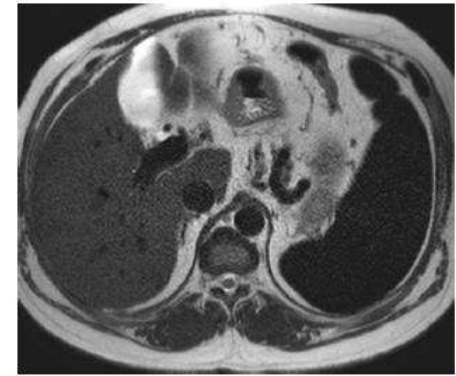


Figure 3. Axial T2-weighted single-shot image through the liver and spleen demonstrates hypointensity in the spleen due to the T2 shortening effect from iron accumulation. Ferumoxytol is taken up by the reticuloendothelial system, presumably resulting in the observed iron accumulation.

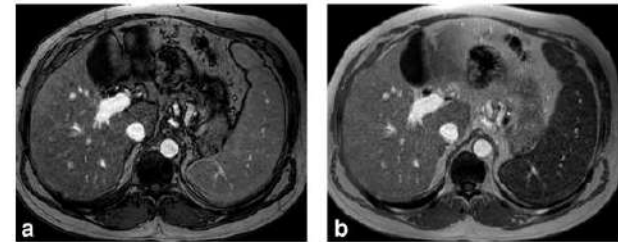


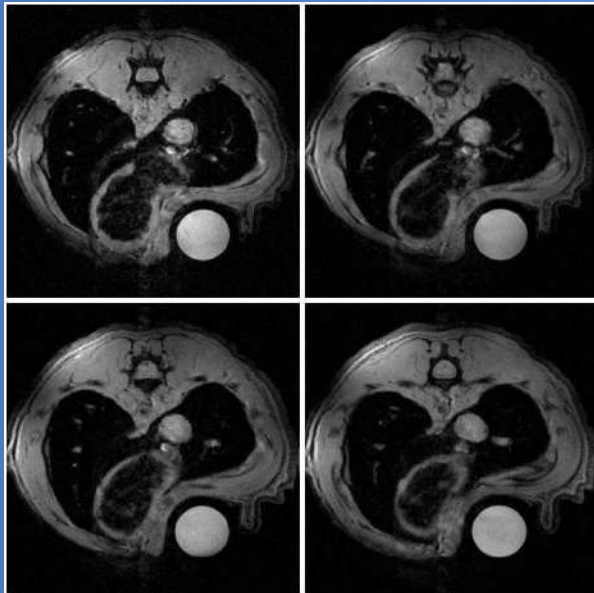
Figure 4. Axial out-of-phase image (TE 2.3 msec), prior to GBCA administration, shows T1 hyperintensity in the blood pool (a). Axial in-phase image (TE 4.6 msec) shows pronounced signal dropout in the spleen due to the T2* effect from iron accumulation, presumably from ferumoxytol uptake (b). No significant signal loss is observed in the liver on the in phase image, indicating little or no ferumoxytol uptake.

DIAGNOSTICS

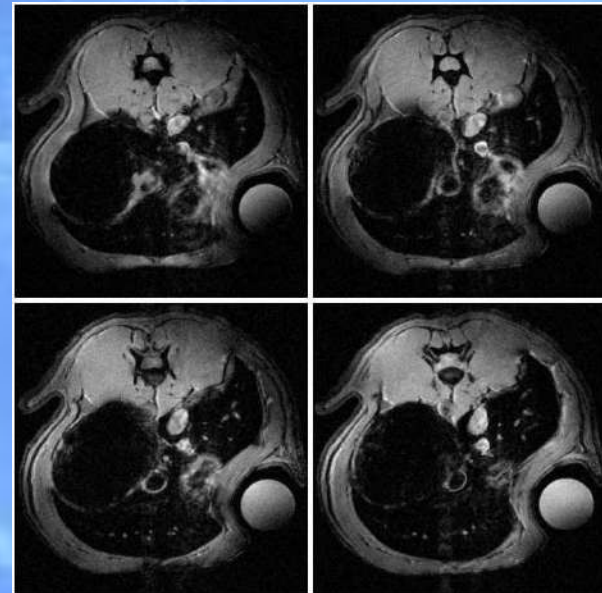
one of ∞ examples of non-specific CA

MRI with Co-ferrites (Colorobbia)

liver of normal rats, at 1 day from the bolus injection



Endorem
vs
Co-ferrites



Even just our group collaborated with several researchers synthesizing **novel MNPs** with **high transverse relaxivity** (i.e. efficiency in MRI image contrast)

until 8 times the (ex-)commercial compound Endorem

Other images about targeting and ... shape

Review

CONTRAST MEDIA & MOLECULAR IMAGING

Received: 11 October 2014; Revised: 30 January 2015; Accepted: 6 February 2015; Published online in Wiley Online Library: 16 April 2015

(wileyonlinelibrary.com) DOI: 10.1002/cmml.1638

Superparamagnetic iron oxide nanoparticles for *in vivo* molecular and cellular imaging

Shahriar Shariff^{a†}, Hajar Seyednejad^{b†}, Sophie Laurent^{c,d*}, Fatemeh Atyabi^e, Amir Ata Saei^{e,f} and Morteza Mahmoudi^{e,g,h*}

NANO LETTERS

Letter

pubs.acs.org/NanoLett

Water-Dispersible Ferrimagnetic Iron Oxide Nanocubes with Extremely High r_2 Relaxivity for Highly Sensitive *In Vivo* MRI of Tumors

Nohyun Lee,^{†,§} Yoonseok Choi,^{*,§} Youjin Lee,[†] Mihyun Park,[†] Woo Kyung Moon,[‡] Seung Hong Choi,^{*,‡} and Taeghwan Hyeon^{*,†}

* Single Chain Antibody Fragments

* Nude mouse with melanoma

* Cube

ScFvEGFR-IO

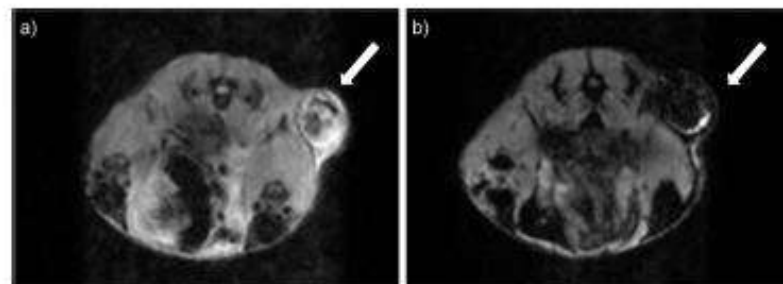
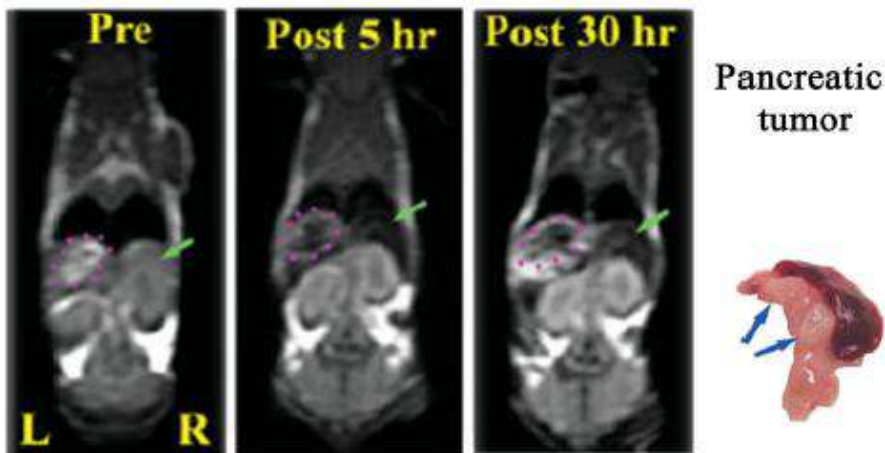


Figure 4. *In vivo* MR Images of the tumor site before (a) and 1 h after (b) intravenous injection of WFIONs (arrows indicate the tumor sites). After administration of WFIONs, the MR signal of the tumor is significantly attenuated.

Other images about targeting

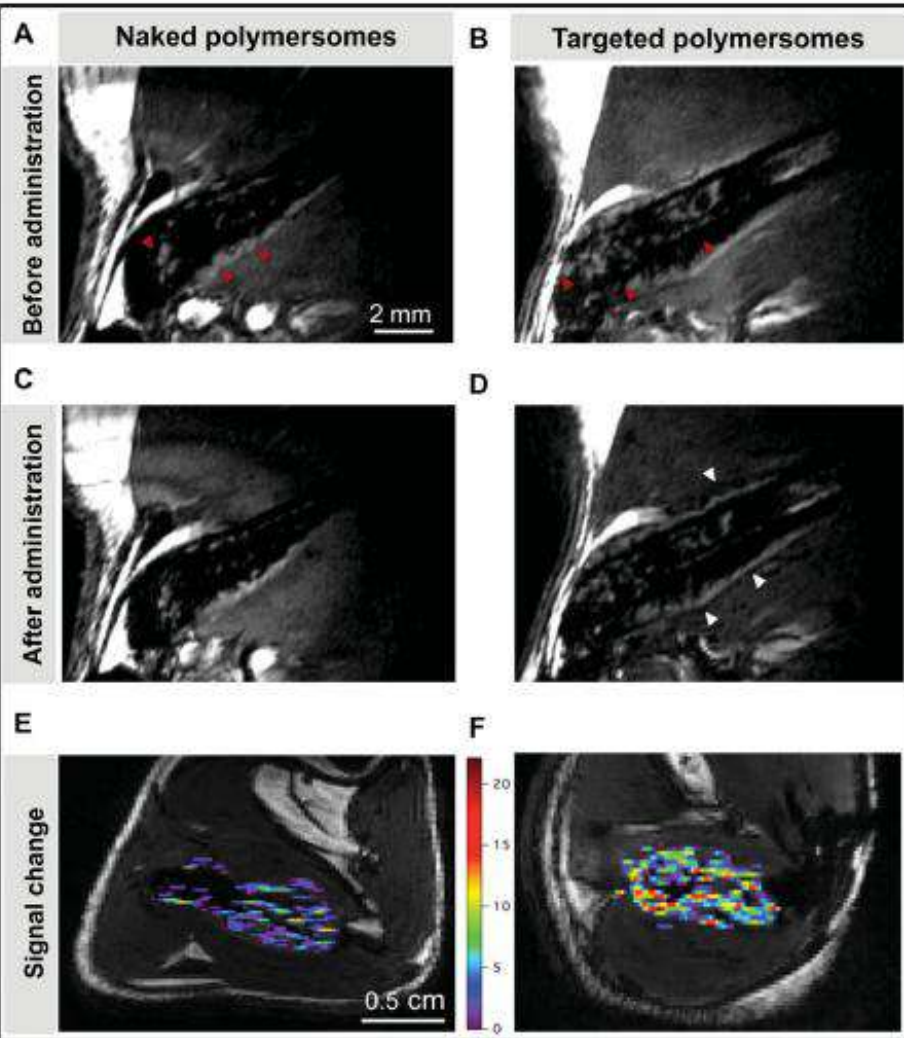


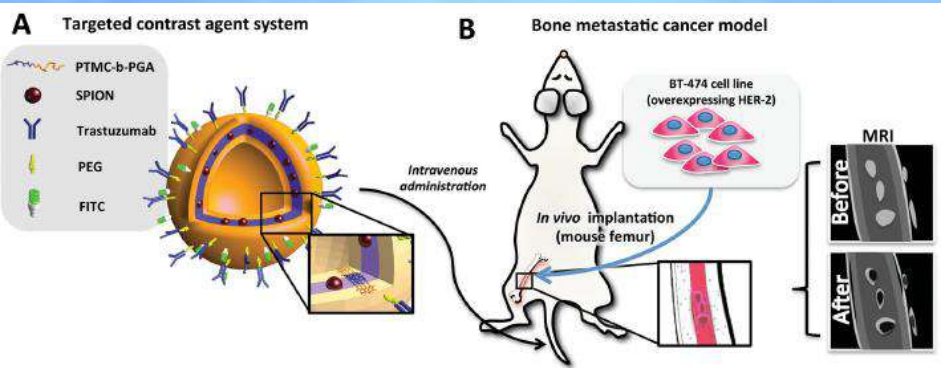
Figure 3. Bone BT-474 tumor targeting as assessed from high resolution 3D TrueFisp MRI. Extracted axial views and color map of relative signal change in percent brought by the injection of naked (A) or targeted (B) polymersomes. Longitudinal views before (C,D) and after (E, F) injection of naked (C, E) and targeted (D, F) polymersomes. Red arrows denote tumor tissue. White arrows denote contrast variations on tumor boundaries. Experiments were performed when the tumors reached a volume of 12 to 15 μ l.

ADVANCED
HEALTHCARE
MATERIALS
www.advhealthm.at.de

Materials
Views
www.MaterialsViews.com

Antibody-Functionalized Magnetic Polymersomes: In vivo Targeting and Imaging of Bone Metastases using High Resolution MRI

Line Pourtau, Hugo Oliveira, Julie Thevenot, Yali Wan, Alain R. Brisson, Olivier Sandre, Sylvain Miraux, Eric Thiaudiere,* and Sébastien Lecommandoux*



within
EU- FP7-Nanother

TARGETING: a different approach

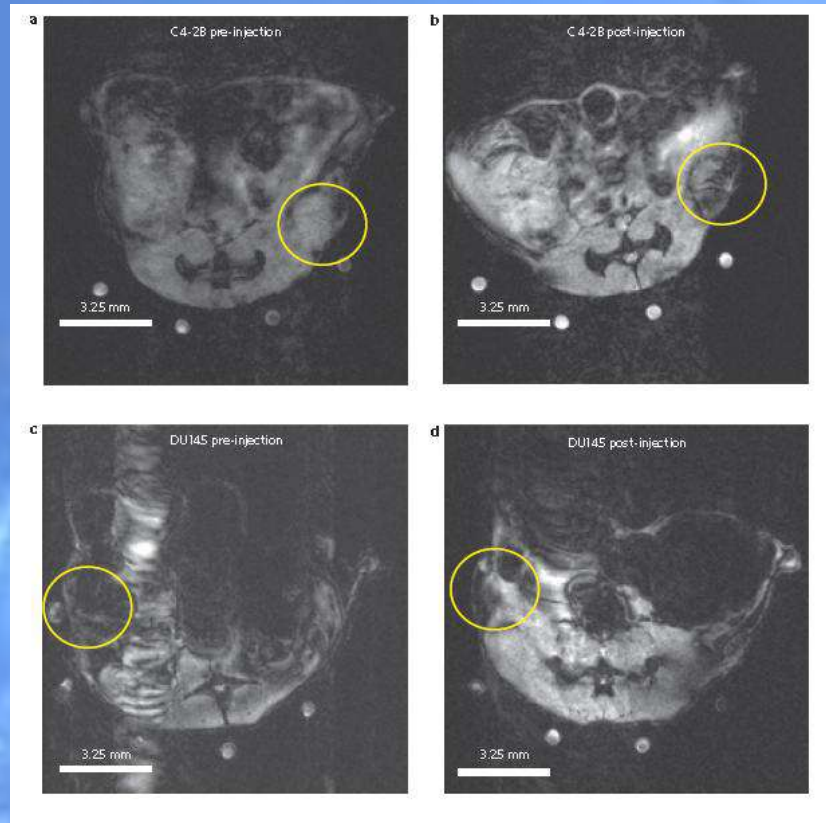
Bacteriophage as a scaffold for MNPs

Ghosh et al.

Modified M13 filamentous bacteriophage with MNPs ($r_2 = 35 \text{ mM}^{-1}\text{s}^{-1}$) and a targeting peptide

Target : SPARC glycoprotein

C4-2B prostate cancer cell line



C4-2B

DU145
(negative control)

Figure 3 | Targeting *in vivo* using MRI and correlative histology. **a,b**, MR scans of mice with C4-2B tumours (encircled) pre-injection and 24 h post-injection, respectively, with M13-SBP-MNP. **c,d**, MR scans of DU145 control tumours (circled) pre-injection and 24 h post-injection with probe, respectively. Note the maintenance of the bright image of the tumour (circled) in DU145 pre- to post-injection, whereas a post-injection dark contrast against the pre-injection bright MR image is observed in C4-2B (circled). All tumours formed subcutaneously in athymic nude mice and were imaged using a 7 T small animal MR

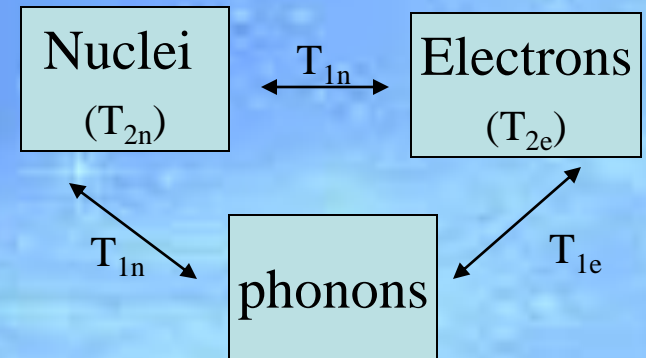
Going toward fundamental physics

NMR TECHNIQUE

EXPERIMENTAL PARAMETERS

3 main parameters:

- spectrum
- nuclear spin-spin relaxation time T_2
- nuclear spin-lattice relaxation time T_1



LOCAL PROBE

- Nuclei are **local probes** \Leftrightarrow sensitive to **local hyperfine interactions**
- **Local spin dynamics (mainly T_1 and T_2) and spin distribution (mainly spectra)** can be studied

In MRI and relaxometry, sensitivity to spin dynamics and molecular “motion”

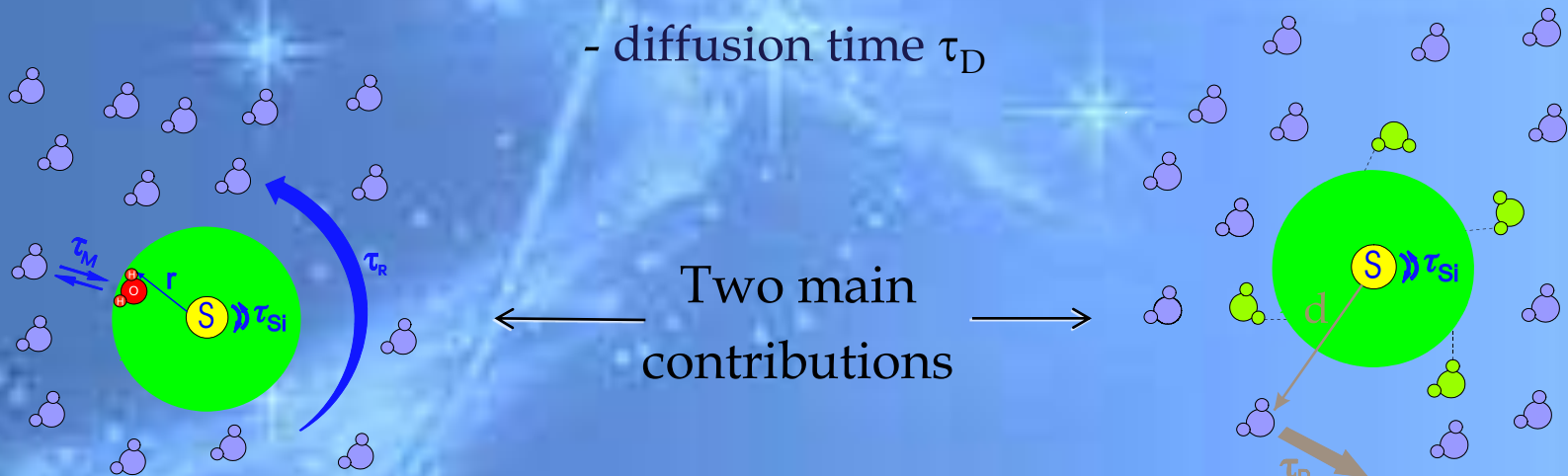
Nuclear Relaxation Mechanisms

$$R_{1,2,oss} = \frac{1}{T_{1,2,d}} + \frac{1}{T_{1,2,inner}} + \frac{1}{T_{1,2,outer}}$$

$$1/T_{1,2} = f(\gamma_e, \gamma_n, \omega_L^e, \omega_L^n, \tau_{S1,2}, \tau_R, \tau_M, q, r, \tau_{S0}, \dots)$$

Several correlation times within the game :

- Chemical exchange time of coordinated water τ_M
- rotational time (brownian) τ_R
- electronic relaxation time (also Neel reversal) τ_{Si}
- diffusion time τ_D

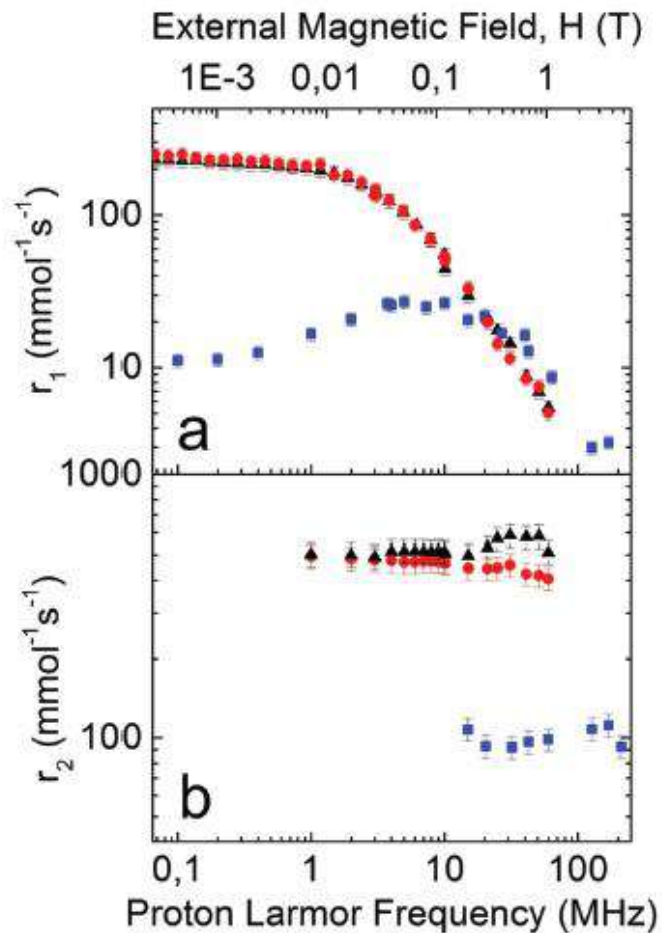


Inner Sphere (IS)

Outer Sphere (OS)

Colloidal assemblies of oriented maghemite nanocrystals and their NMR relaxometric properties†

Athanasia Kostopoulou,^a Sabareesh K. P. Velu,^b Kalaivani Thangavel,^b Francesco Orsini,^b Konstantinos Brintakis,^{a,c} Stylianos Psycharakis,^{a,d} Anthi Ranella,^a Lorenzo Bordonali,^e Alexandros Lappas^{*a} and Alessandro Lascialfari^{*b}



Assemblies of oriented
maghemite nanocrystals

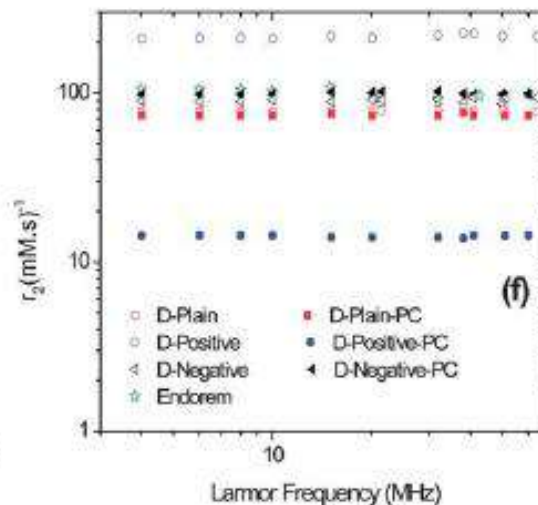
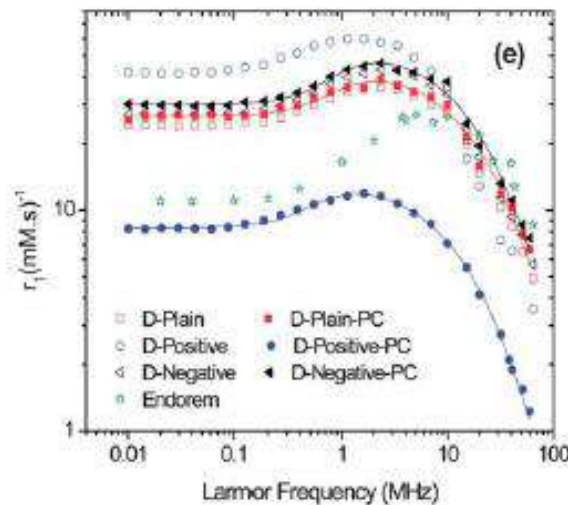
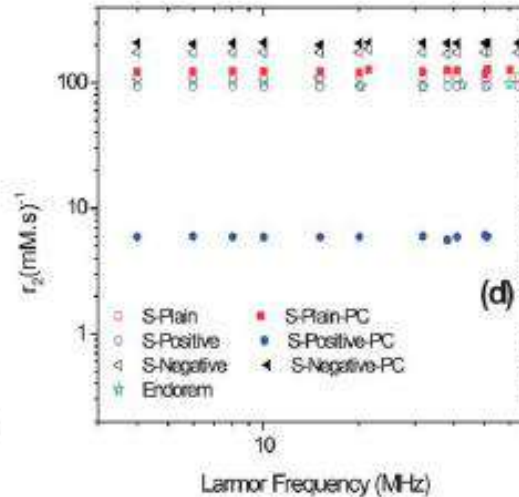
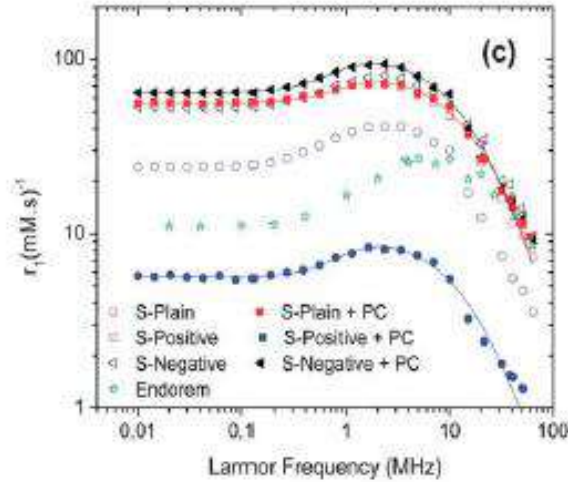
$r_2 > 400\text{-}500 \text{ mM}^{-1}\text{s}^{-1}$!!!

Other exp. results

Protein corona affects the relaxivity and MRI contrast efficiency of magnetic nanoparticles†

Houshang Amiri,^{*a} Lorenzo Bordonali,^e Alessandro Lascialfari,^{ef} Sha Wan,^b Marco P. Monopoli,^b Iseult Lynch,^{†*b} Sophie Laurent^g and Morteza Mahmoudi^{*cd}

Cite this: *Nanoscale*, 2013, 5, 8656



$r_2 > 100-200 \text{ mM}^{-1}\text{s}^{-1}$

Protein corona
affects r_2 !!

* Plain \Rightarrow no

* " - " charge \Rightarrow slight increase

* " + " < charge \Rightarrow decrease

Magnetic Fluid Hyperthermia (MFH)

..... after and/or trying to go beyond
Jordan's clinical studies

OPEN ACCESS Freely available online

PLOS ONE

Design Maps for the Hyperthermic Treatment of Tumors with Superparamagnetic Nanoparticles

Antonio Cervadoro^{1,2}, Chiara Givero³, Rohit Pande^{4,5}, Subhasis Sarangi⁵, Luigi Preziosi³, Jarek Wosik^{4,5}, Audrius Brazdeikis^{5,6}, Paolo Decuzzi^{1,7*}

1 Department of Translational Imaging, The Methodist Hospital Research Institute, Houston, Texas, United States of America, 2 Department of Mechanics, Politecnico di Torino, Turin, Italy, 3 Department of Mathematical Sciences, Politecnico di Torino, Turin, Italy, 4 Department of Electrical and Computer Engineering, University of Houston, Houston, Texas, United States of America, 5 Texas Superconductivity Center, Houston, Texas, United States of America, 6 Department of Physics, University of Houston, Houston, Texas, United States of America, 7 Department of Experimental and Clinical Medicine, University of "Magna Graecia", Catanzaro, Italy

Theranostics 2012, 2(1) 113

IVYSPRING INTERNATIONAL PUBLISHER

Theranostics
2012, 2(1):113-121. doi: 10.7150/tno.3854

Research Paper

Magnetic Nanoparticle-Based Hyperthermia for Head & Neck Cancer in Mouse Models

Qun Zhao^{1,2*}, Luning Wang^{1,2}, Rui Cheng³, Leidong Mao³, Robert D. Arnold⁴, Elizabeth W. Howerth⁵, Zhuo G. Chen⁷, and Simon Platt⁶

Balivada et al. BMC Cancer 2010, 10:119
<http://www.biomedcentral.com/1471-2407/10/119>

BMC Cancer

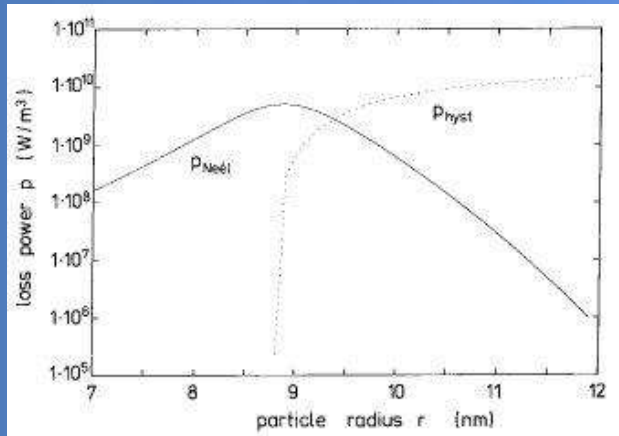
RESEARCH ARTICLE Open Access

A/C magnetic hyperthermia of melanoma mediated by iron(0)/iron oxide core/shell magnetic nanoparticles: a mouse study

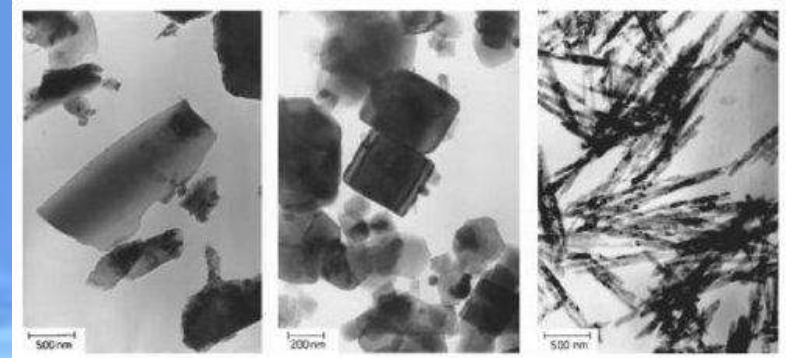
Sivasai Balivada¹, Raja Shekar Rachakatla¹, Hongwang Wang³, Thilani N. Samarakoon³, Raj Kumar Dani³, Maria Pyle¹, Franklin O. Kroh², Brandon Walker², Xiaoxuan Leaym², Olga B. Koper², Masaaki Tamura¹, Viktor Chikan³, Stefan H. Bossmann³, Deryl L. Troyer^{1*}

MFH: Iron/M oxide nanoparticles

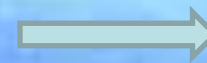
Dimensions



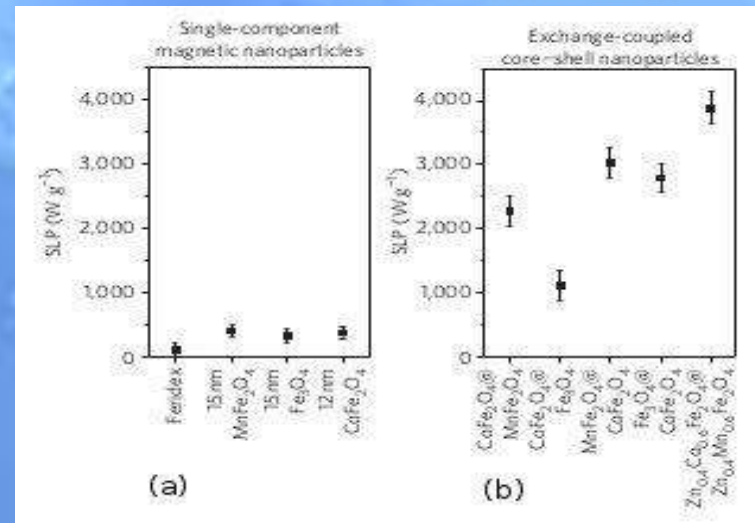
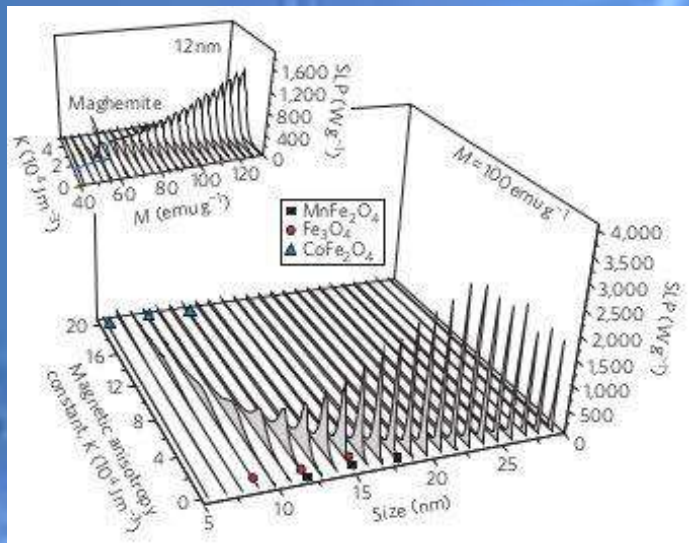
Shape



Optimization of K, M and D in core-shell NPs



High SLP



Starting from the end ...

Jordan et al. @ Charité Universitätsmedizin Department of Radiotherapy

J Neurooncol (2011) 103:317–324
DOI 10.1007/s11060-010-0389-0

CLINICAL STUDY – PATIENT STUDY

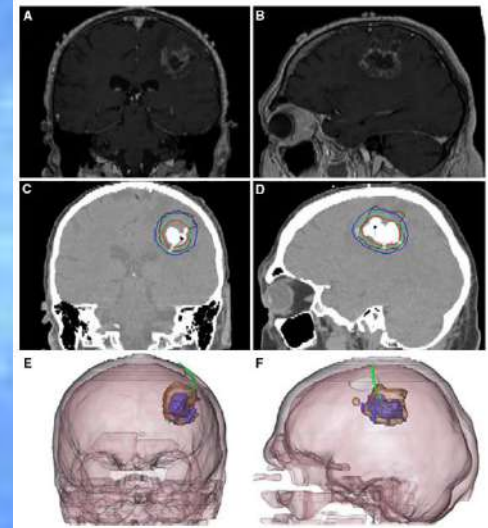
Efficacy and safety of intratumoral thermotherapy using magnetic iron-oxide nanoparticles combined with external beam radiotherapy on patients with recurrent glioblastoma multiforme

Klaus Maier-Hauff · Frank Ulrich · Dirk Nestler ·
Hendrik Nitsch · Peter Wust · Burghard Thiesen ·
Helmut Orawa · Volker Bodach · Andreas Jordan

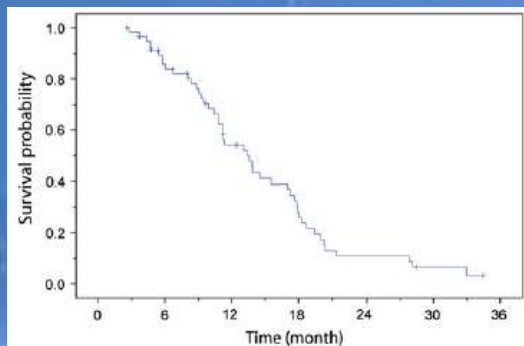
After diagnosis of first tumor recurrence/progression

Table 1 Patient characteristics (n = 59)

	No.	(%)
First-line therapy		
Resection	56	95
Radiotherapy	58	98
Chemotherapy	51	86
Patients with prior treatment following tumor recurrence but before study entry	24	41
Resection	11	19
Radiotherapy	2	3
Chemotherapy	17	29
KPS at study entry—median (range)	90 (60–100)	
Karnofsky performance score (KPS) ≥80	46	78
Age in years at study entry—median	55.7	
Patients with age <50	23	39
Patients with age ≥50	36	61



Thermo-/radiotherapy combination



Results:

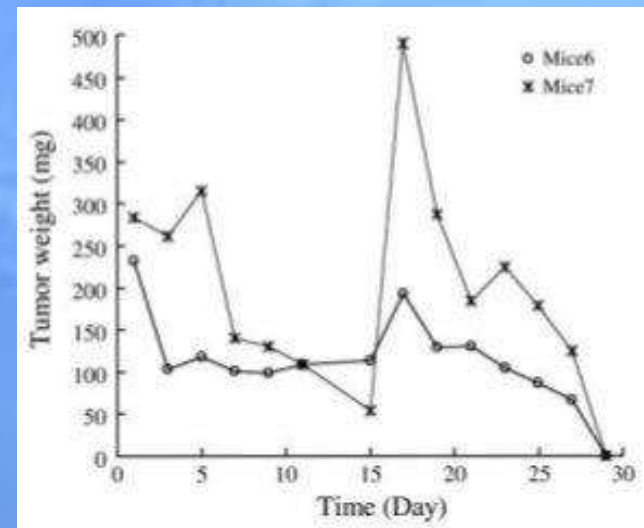
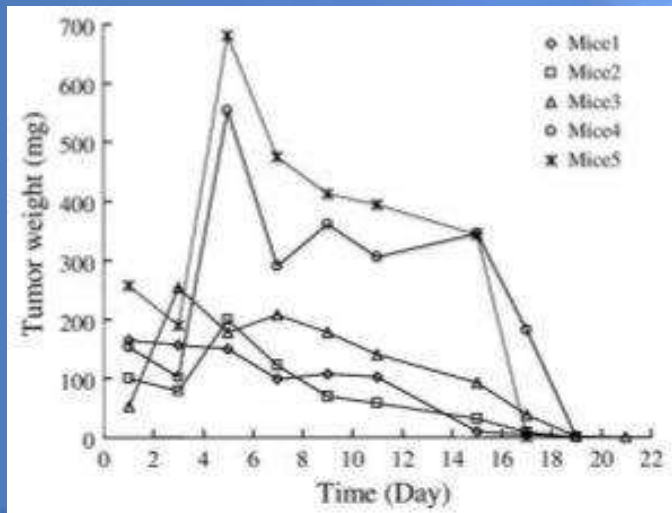
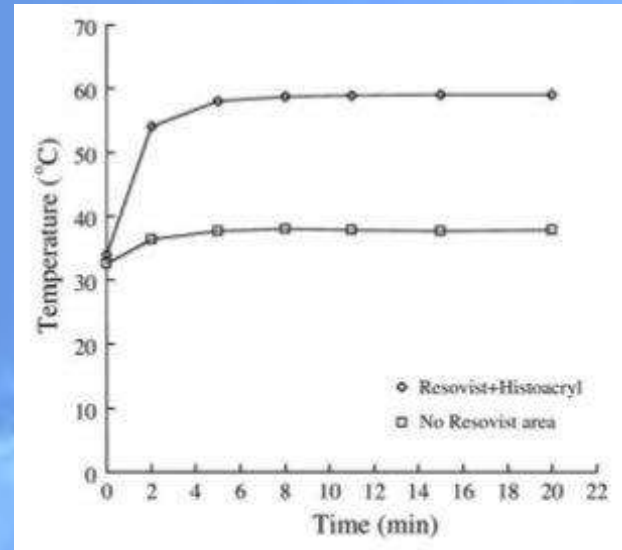
- **Increase** in median OS-2 -> **7.2 months**
- **Increase** in median OS-1 -> **8.6 months**
- Few side effects

major Drawbacks observed:

- no MRI after treatment
- no metallic materials < 40cm treated area

MFH: Resovist® (commercial product)

- SPION CA for MRI
- Diameter magnetic core: 9 nm
- Diameter nanoparticle: 62 nm (core + carboxydextran)
- 62,1 kHz, 2,2 kW
- Tumour CT-26 (murine colon)



Tendency to diminution of tumour volume

MFH: a different type of MNPs

6 different kind of nanoparticles including magnetosomes

- Tumour cells MDA-MB-231 (breast)
- 40 mT
- 183 kHz

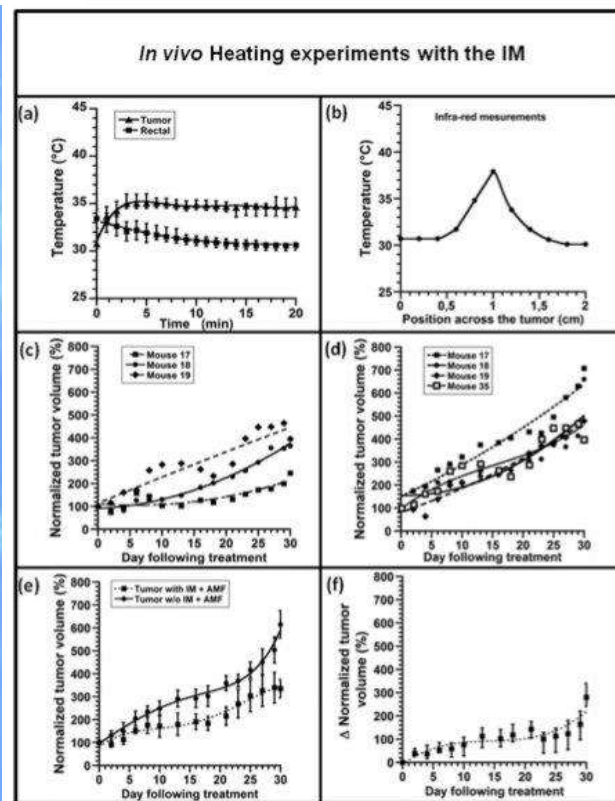
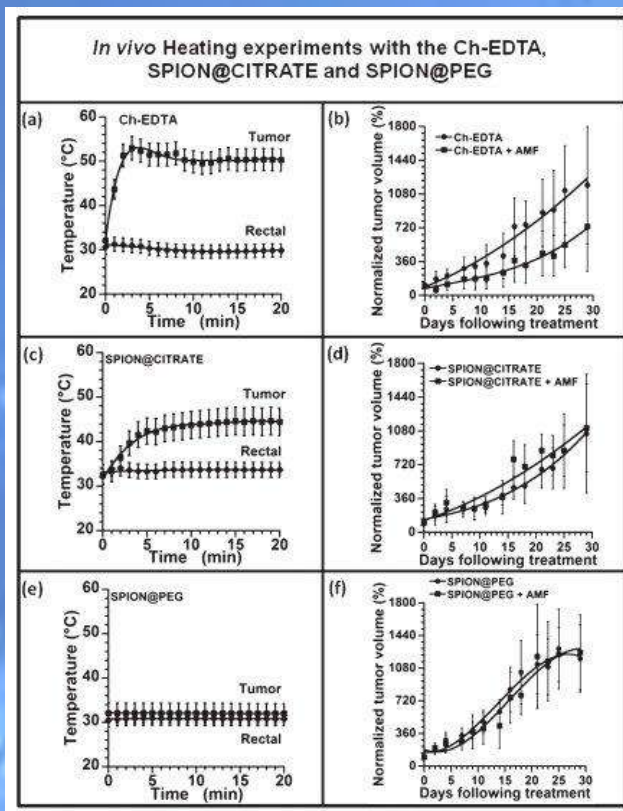
Alphandery et al.

VOL. 5 ■ NO. 8 ■ 6279-6296 ■ 2011

ACS NANO
www.acsnano.org

- 20 minutes
- From AMB-1 magnetotactic bacteria
- 3 treatments (alternate days)
- SAR Ch-Std: 390 W/g

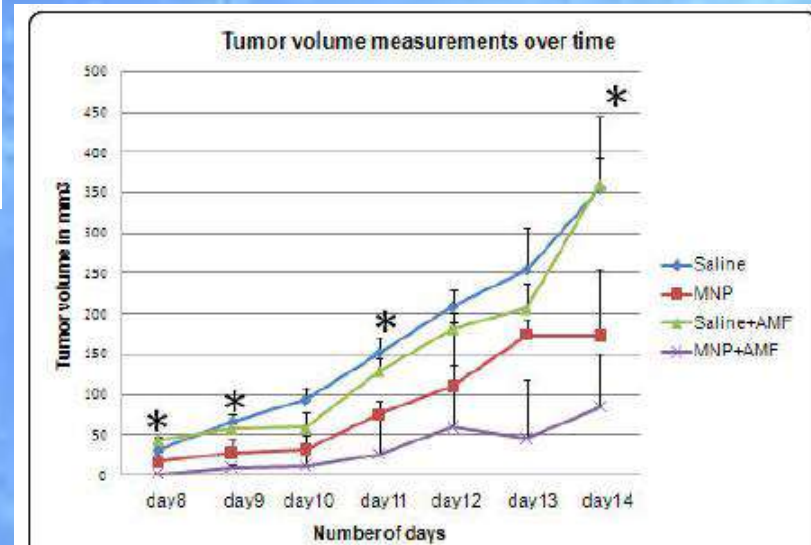
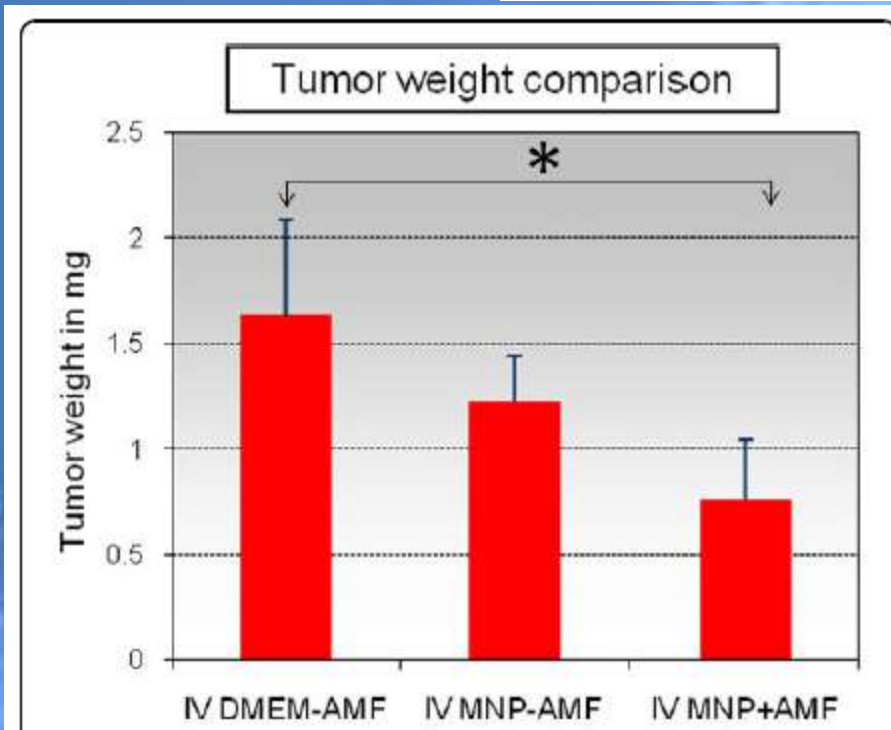
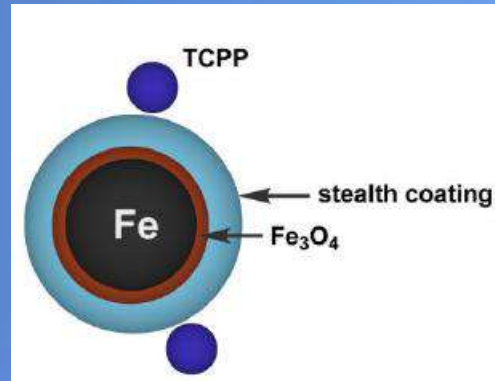
!!! Chains magnetosomes !!!



In 1 case the tumour disappear

MFH: core-shell nanoparticles

- Core of Fe and coating of Fe_3O_4
- 12 ± 3 nm
- 5 kA/m, 366 kHz
- SAR = 64 W/g
- Melanoma cells B16-F10
- $\Delta T = 11^\circ\text{C}$



The tumour volume
increase rate **slows down**

An example of collaboration

TD COST Action TD1402

Management Committee

MC Chair	TBA
MC Vice Chair	TBA

■ Data registration in e-COST pending subject to online registration and nomination acceptance by nominee.

COST Participants

Country	MC Member
Austria	▶ Ms Sonja HARTL
Belgium	▶ Dr Simo SPASSOV
Belgium	▶ Prof Luc DUPRE
Cyprus	▶ Dr Petri PAPAPHILIPPOU
Czech Republic	▶ Dr Daniel HORAK
Denmark	▶ Mr Mikkel FOUGT HANSEN
Denmark	▶ Dr Cathrine FRANDSEN
France	▶ Dr Olivier SANDRE
France	▶ Prof Claire BILLOTEY
Germany	▶ Dr Silvio DUTZ
Germany	▶ Prof Christoph ALEXIOU
Greece	▶ Dr Aristides BAKANDRITSOS
Greece	▶ Prof George LOUDOS
Hungary	■ Prof Beika TOMBACZ
Ireland	▶ Dr Oliviero GOBBO
Ireland	■ Dr Dermot BROUGHAM
Italy	▶ Prof Alessandro LASCIALFARI
Italy	▶ Dr Claudio SANGREGORIO
Norway	■ Prof Kenneth D. KNUDSEN
Portugal	▶ Dr Sofia COSTA LIMA
Portugal	▶ Dr Maria De Deus CARVALHO
Romania	▶ Dr Ladislau VEKAS
Romania	▶ Dr Rodica Paula TURCU
Serbia	▶ Dr Madan KUSIGERSKI
Slovakia	▶ Dr Vlasta ZAMSOVA
Slovakia	▶ Prof Peter KOPCANSKY
Spain	▶ Dr Daniel ORTEGA
Spain	■ Fernando PLAZAOLA MUGURUZA
Sweden	▶ Prof Christer JOHANSSON
United Kingdom	▶ Prof Thanh Thi Kim NGUYEN
United Kingdom	▶ Mr Carlton JONES

Trans-Domain COST Action TD1402

- ▶ Description
- ▶ Parties
- ▶ Management Committee

General Information¹

Science officer of the Action:
[Dr María MORAGUES CANOVAS](#)
 Administrative officer of the Action:
[Ms Anja VAN DER SNICKT](#)

Downloads¹

Action Fact Sheet
[Download AFS as .RTF](#)
 Memorandum of Understanding
[Download MoU as PDF](#)

Websites¹

Domain website:
<http://www.cost.eu/tdp>

¹ content provided by e-COST.
 Data is synchronised once per night.



Home | Domains and Actions | Trans-Domain Proposals | Actions | TD1402

TD COST Action TD1402

Multifunctional Nanoparticles for Magnetic Hyperthermia and Indirect Radiation Therapy (RADIOMAG)

Descriptions are provided by the Actions directly via e-COST.

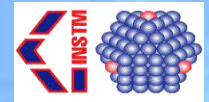
The Action aims to bring together and to organise the research outcomes from the different participating network members in a practical way to provide clinicians with the necessary input to trial a novel anti-cancer treatment combining magnetic hyperthermia and radiotherapy, also identifying future research objectives upon appraisal of the obtained results. Feedback between the different working groups here is essential, and is expected that the lifetime of this Action proposal will eventually result in a compendium of best practices for magnetic hyperthermia.

RADIOMAG will generate new and strengthen the existing synergies between technical advances (thermal imaging / MH), new treatment concepts (combined targeting radiosensitisation and magnetic thermotherapy) and biocompatible coating in order to achieve a breakthrough in the clinical application of magnetic hyperthermia. Due to the complexity of this aim, synergies can only be achieved on a longer time frame, by means of workshops, STSMs, joint publications, common Horizon 2020 research proposals and exchange with other COST Actions (e.g. TD1004, TD1205).



FP7 - NANOTHER project

System tested: INSTM-COLORITA



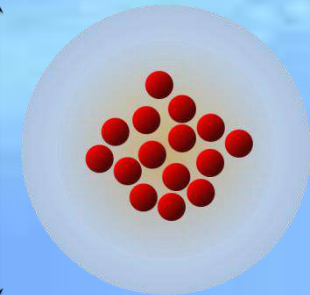
Sample 15_Block-M (115/15) - average diameter $d = 130 \pm 30$ nm

Core : magnetite. Block-M copolymer coating. Functions : drug &/or folic acid

* All samples with Paclitaxel (PTX)

* Two classes : **with and without folic acid** (folic acid is the targeting agent)

Formulation Description	Composition (w/v):	About 8 ml (exactly 10 mg/ml) Hybrid IS19b (Argus) – Magnetite (Colorita) NPs
	Pharmaceutical form	Suspension
	Dilution solution	Water



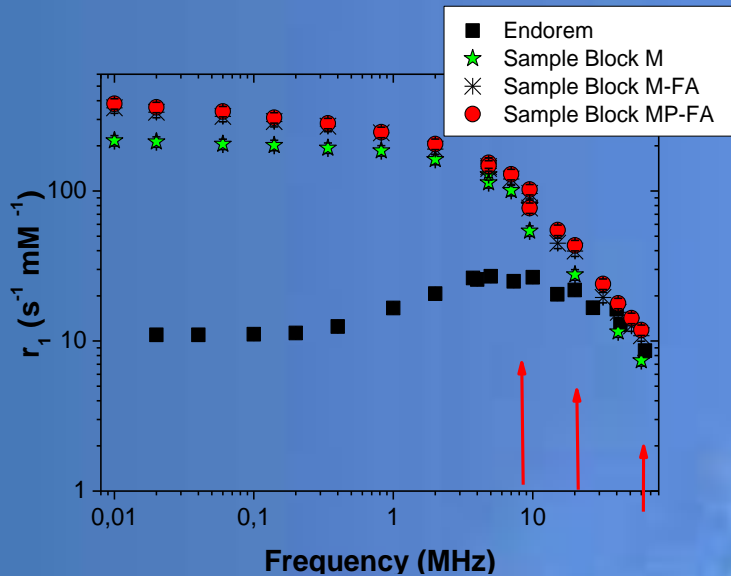
TUMOUR MODEL (developed BY Leitat)

* Ten female homozygote nude mice

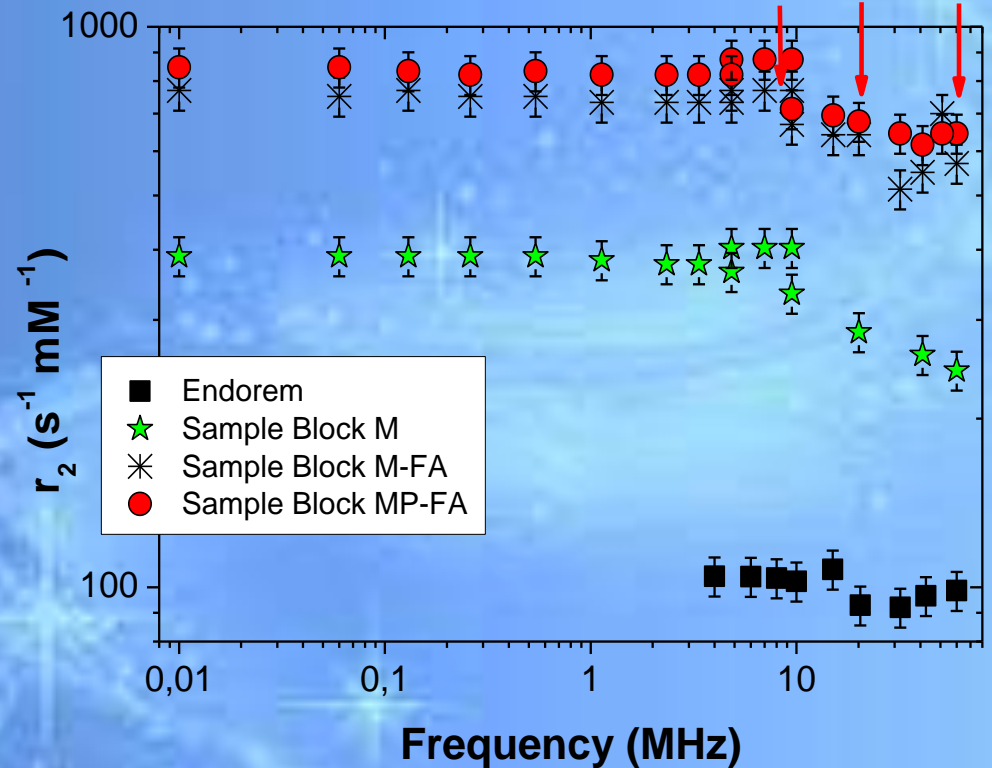
* **MDA-MB-231 human breast cancer**, over-expressing folate receptors

* **Subcutaneous** implantation

Relaxometry



Hybrids Fe ₃ O ₄ (also Paclitaxel)		
	d	r _{HYD}
BLOCK-M	12	~130
BLOCK-MP	12	~130
BLOCK-MP_FA	12	~150



BLOCK-MP-FA good r_2 relaxivity compared to commercial compound Endorem.

Promising for applications as negative MRI contrast agent (also with Paclitaxel) :

8 times higher relaxivity ! ⇒ GO ON!!!

in vivo MRI protocol

INSTM-COLORITA 15_Block-M-FA (115/15)

Mice investigated : total 10

* 2 animals with intratumoral injection of NPs with folic acid **WITHOUT** MFH treatment

* 3 animals with intratumoral injection of NPs with folic acid **WITH** MFH treatment

The above 5 animals will be sacrificed when tumour reaches 2 cc. Liver, kidneys, spleen, tumour will be excised.

* 1 animal with slow infusion of NPs with folic acid to see **targeting** at 2, 24 and 48 hrs

* 1 animal with slow infusion of Endorem to see **targeting** at 2, 24 and 48 hrs

* 1 animal with slow infusion of NPs with folic acid to see **targeting** at 2, 24 hrs (to be sacrificed for histological control)

* 1 animal with slow infusion of Endorem to see **targeting** at 2, 24 hrs (to be sacrificed for histological control)

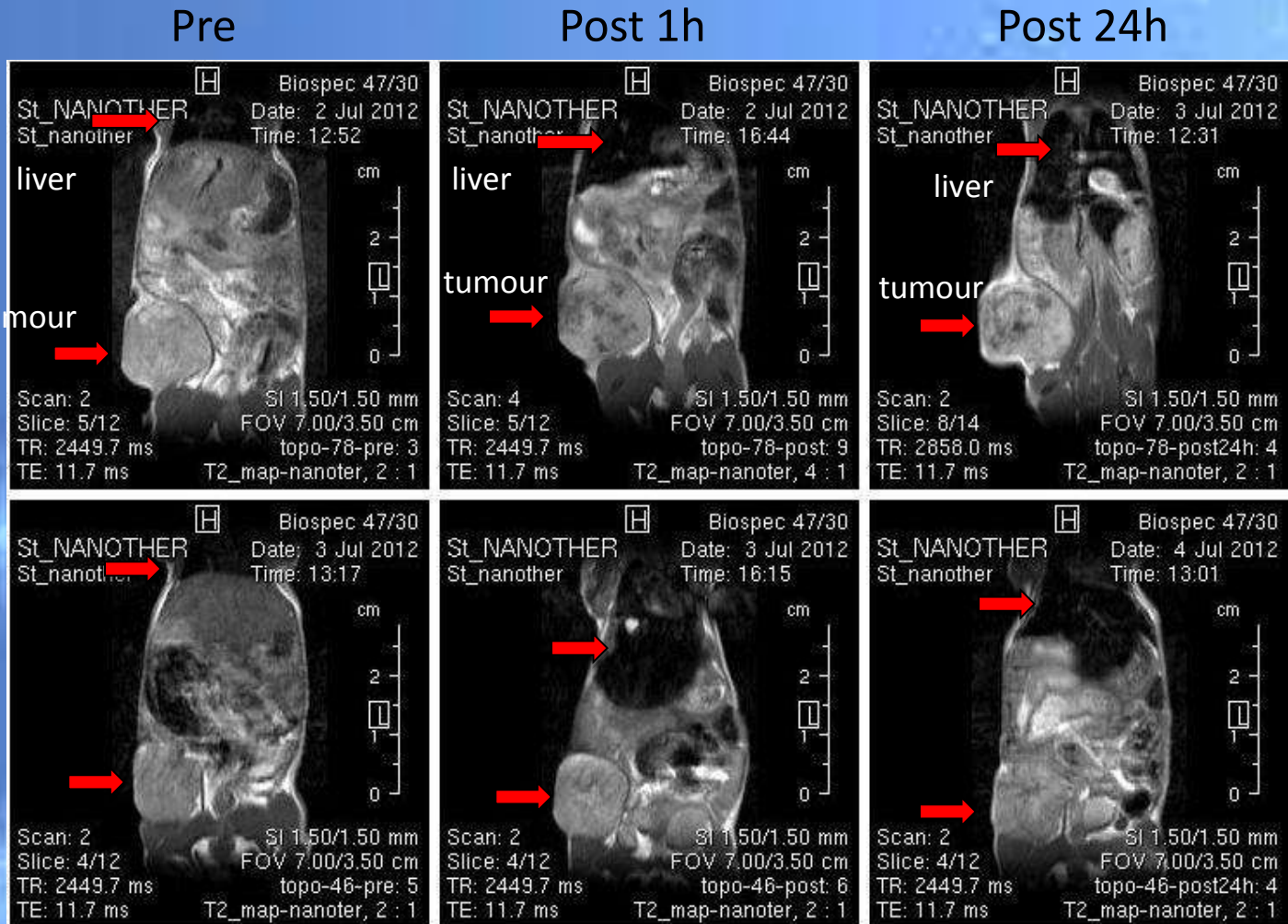
* 1 animal with slow infusion NPs without folic acid to see **targeting** at 2, 24 hrs

Biodistribution

SAGITTAL T2W IMAGES - with folic acid

NPs with
folic acid

tumour



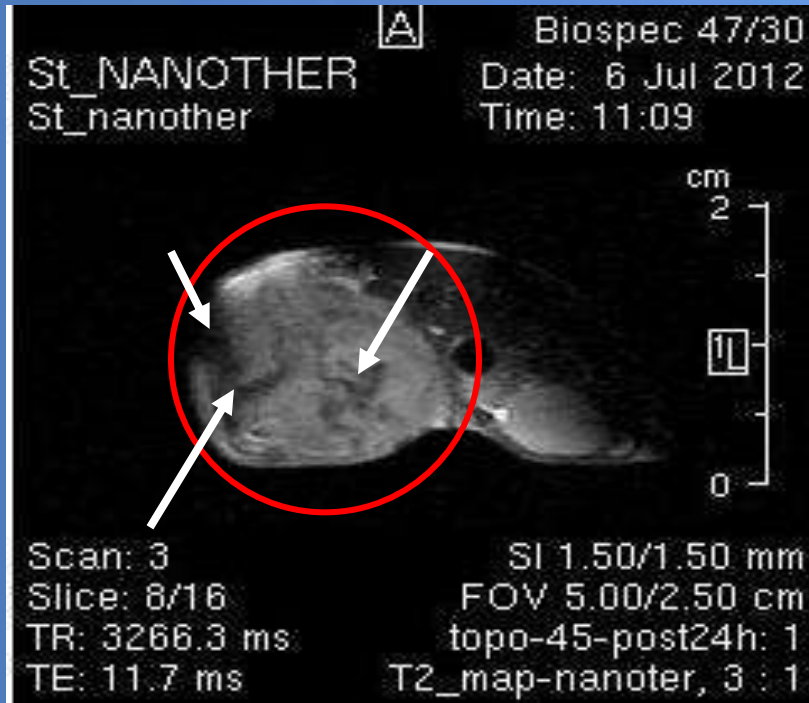
**MOSTLY
IN LIVER**

Endorem

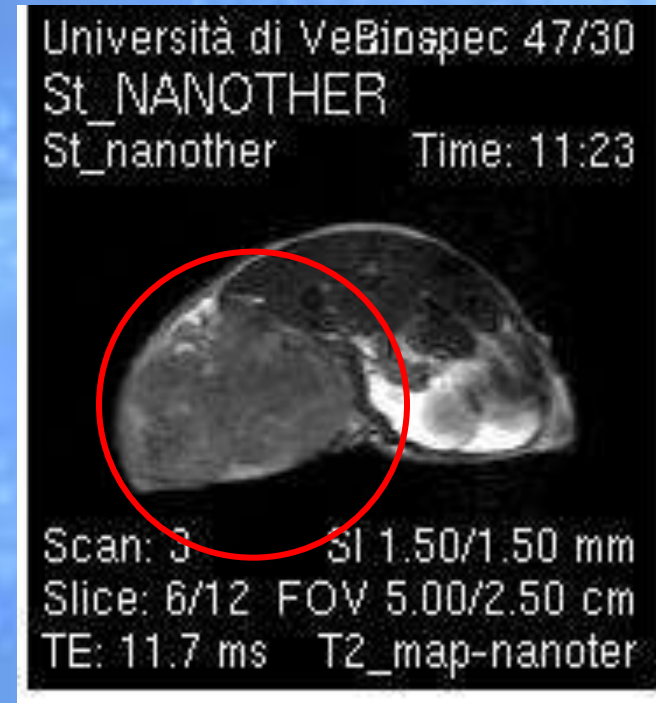
Zoom on targeting

T2W images: post 24h on the tumour

NPs INSTM-Colorita **with folic acid**



NPs **without folic acid**



A semi-quantitative Analysis : T_2 around tumour (to be refined and quantified more properly)

- * Diminishes by 15-20% in NPs with folic acid
- * Diminishes by 3-4% in NPs without folic acid

NPs with folic acid *vs* Endorem[®]

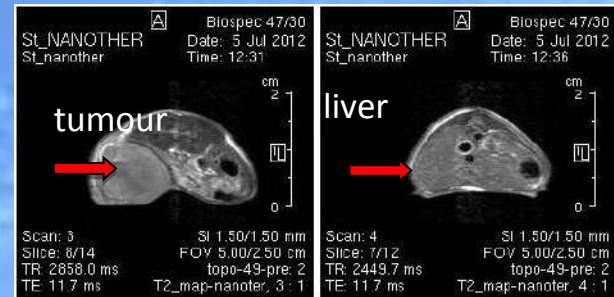
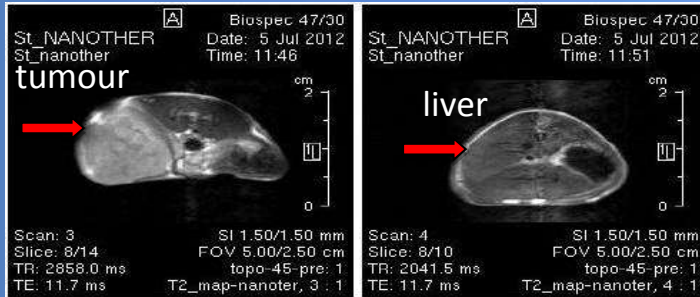
AXIAL T2W IMAGES

slow infusion (400 microliters in 1h, correspondent to 250 micromol/kg)

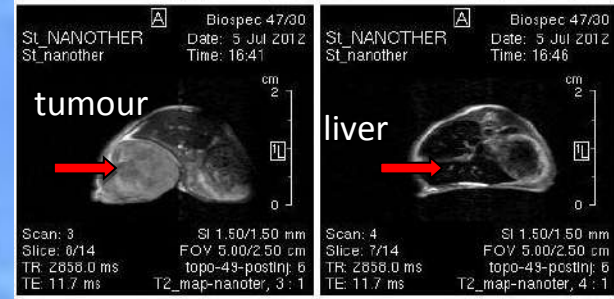
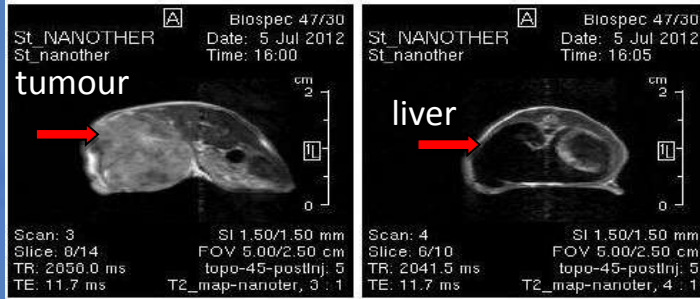
INSTM-Colorita with folic acid (target !)

Endorem (does not target, as expected)

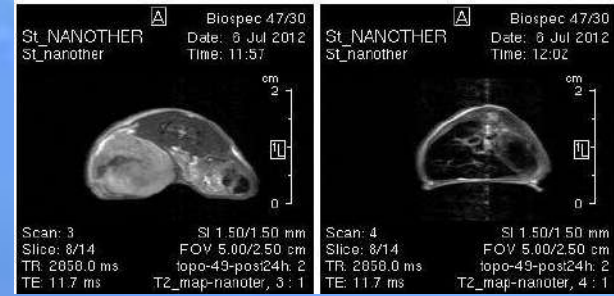
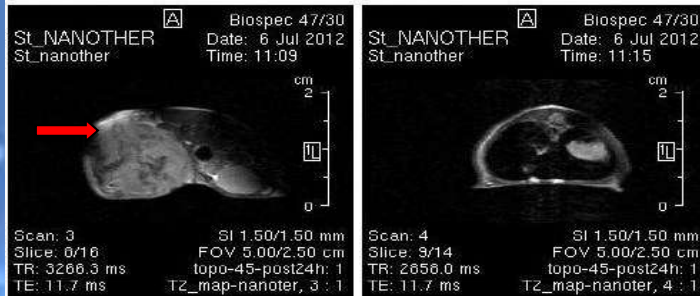
Pre



Post 1h

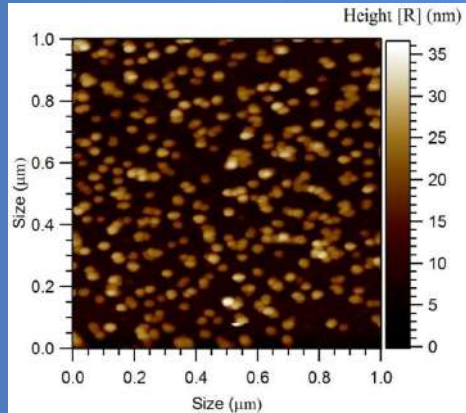


Post 24h

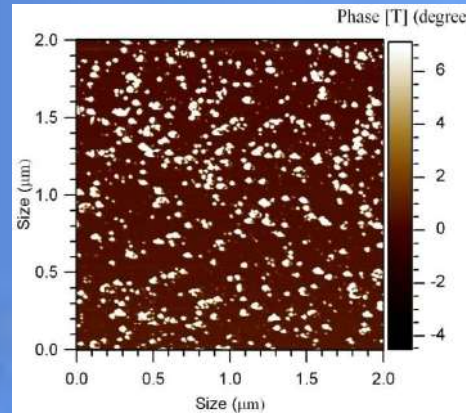


Physico-chemical characterization

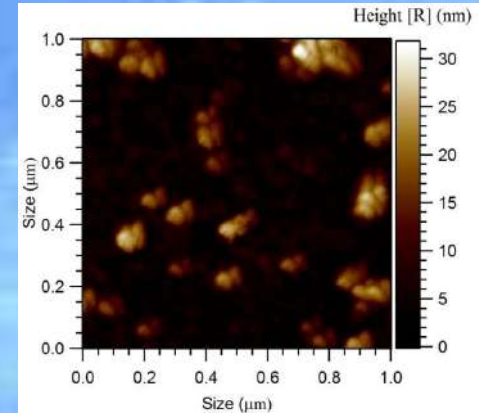
AFM Micrographs



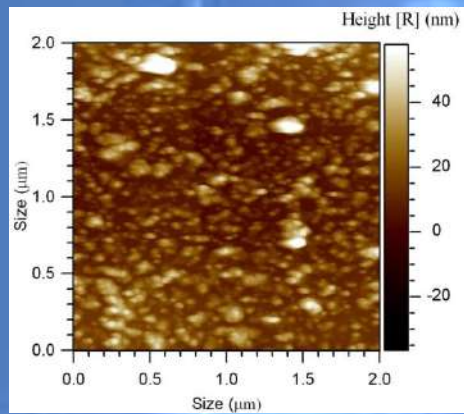
Block-M



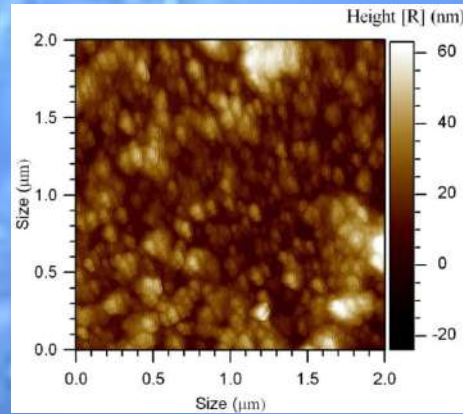
Block-P



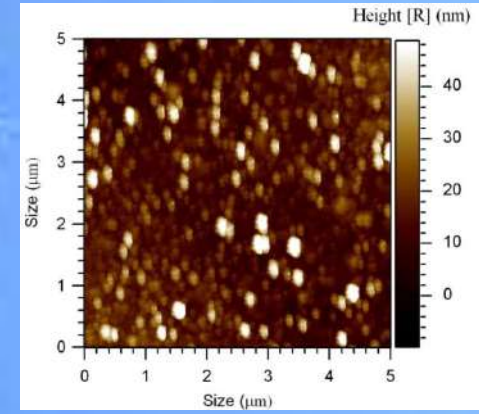
Block-MP



Block-FA



Block-M-FA



Block-MP-FA

Probes: $^1\text{H}-\mu^+$

Measure: relaxation times of
Nuclear Magnetization/ Muon's Polarization

WE MEASURE

The Electronic spectral density

$$J_e(\omega) = \text{FT} [G(\underline{r}, t)]$$

- Interacting with **MNP's** THEY RELAX in $t < s$

$J_e(\omega)$ IS THE PROBABILITY TO FIND AN
ELECTRONIC OSCILLATION AT ω

SIMPLE CASE!!

$$J_A(\omega) = \frac{\tau}{1 + (\omega\tau)^2}$$

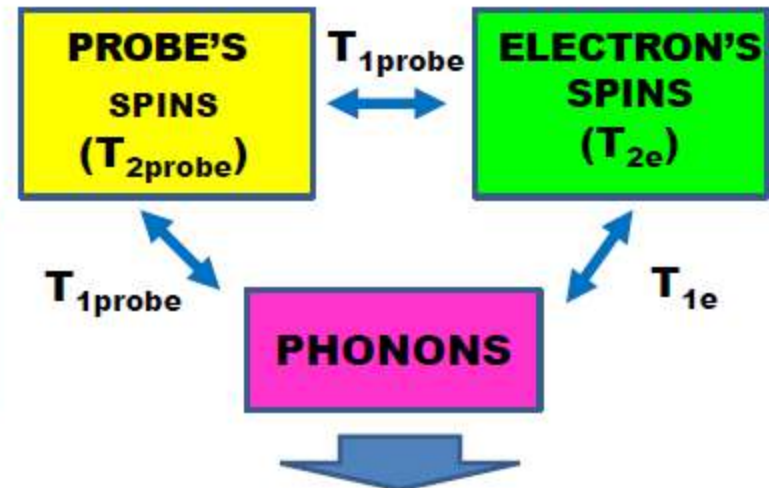
WE WANT

The Electronic correlation function

$$G(\underline{r}, t)$$

$G_e(t)$ DESCRIBES EQUILIBRIUM FLUCTUATIONS OF A QUANTITY F (FIELD)

$$G_{AA}(\tau) = \langle F(0)F(\tau) \rangle = \lim_{T \rightarrow \infty} 1/T \int_0^T F(t)F(t+\tau)dt$$



LONGITUDINAL (SPIN-LATTICE) RELAXATION

$$\frac{1}{T_1}^{Probe} \sim \chi T J_e(\omega_{Probe})$$

TRANSVERSAL (SPIN-SPIN) RELAXATION

$$\frac{1}{T_2}^{Probe} \sim \chi T J_e(0)$$

